Adv Polym Sci
DOI: 10.1007/12_2013_221

Ordering of Polypeptides in Liquid Crystals, Gels and Micelles

Chunhua Cai, Jiaping Lin, Zeliang Zhuang, and Wenjie Zhu

Abstract Ordered structures assembled from polypeptides have attracted a great deal of attention over the past few decades. Both α-helix and β-sheet conformations of polypeptides support the formation of ordered structures during the assembly process. For polypeptides with α-helix conformation, the ordered structures are formed mainly by side-by-side packing of α-helix rods. For polypeptides with β-sheet conformation, ordering of the chains can be achieved by parallel or antiparallel packing. The ordering characteristic of polypeptide chains gives rise to fascinating assembly behaviors of polypeptide homopolymers and copolymers in solution. Usually, a decrease in polymer concentration is accompanied by the assembly of polypeptides into liquid crystals (LCs), gels, and micelles. This review describes the ordering structures of polypeptides in these assemblies. In LC structures, polypeptide homopolymer chains are packed in a highly ordered fashion with smectic, nematic, and cholesteric phases. Both polypeptide homopolymers and copolymers support the formation of gels in solution. The dislocated side-by-side packing of polypeptide helices is the basic ordering characteristic of the polypeptides in gels. Compared with the α-helix conformation, gels formed from polypeptides with β-sheet conformation show higher stability. In dilute solutions, amphiphilic polypeptide copolymers can self-assemble into micelles that include cylinders, vesicles, and complex hierarchical structures. The ordering nature of the polypeptide chains can be observed in the assemblies. The close relationship with proteins makes polypeptides and their assembly structures ideal models for protein research and promising candidates in biorelated applications.

Keywords Gels · Liquid crystals · Micelles · Ordered structure · Polypeptide · Self-assembly

C. Cai, J. Lin (✉), Z. Zhuang, and W. Zhu
Shanghai Key Laboratory of Advanced Polymeric Materials, Key Laboratory for Ultrafine Materials of Ministry of Education, School of Materials Science and Engineering, East China University of Science and Technology, Shanghai 200237, China
e-mail: jlin@ecust.edu.cn

Contents

Abbreviations

AFM	Atomic force microscopy
B	Biphasic region
BD	Brownian dynamics
$CDCl_3$	Deuterated chloroform
$CHCl_3$	Chloroform
DCA	Dichloroacetic acid
DL-PA	Poly(DL-alanine)
DHP	Dendron-helical polypeptide
DMF	*N*,*N*′-dimethylformamide
DP	Degree of polymerization
DPD	Dissipative particle dynamics
EDC	Dichloroethane
I	Isotropic phase
LC	Liquid crystal
L-PA	Poly(L-alanine)
LSCM	Confocal laser scanning microscopy
NCA	*N*-Carboxyanhydride
PArg	Poly(L-arginine)
PBLG	Poly(γ-benzyl L-glutamate)
PClBLA	Poly(β-*p*-chlorobenzyl L-aspartate)
PDI	Polydispersity index
PDMS	Poly(dimethylsiloxane)
PEG	Poly(ethylene glycol)
PEO	Poly(ethylene oxide)
PFS	Poly(ferrocenylsilane)
PHEG	Poly[N^5-(2-hydroxyethyl) L-glutamine]

PIAA	Poly(isocyano-L-alanine-L-alanine)
PIAH	Poly(isocyano-L-alanine-L-histidine)
PLeu	Poly(L-leucine)
PLGA	Poly(L-glutamic acid)
PLL	Poly(L-lysine)
PMLG	Poly(γ-methyl L-glutamate)
PNIPAm	Poly(*N*-isopropylacrylamide)
POM	Polarizing optical micrograph
PPLA	Poly(β-phenethyl L-aspartate)
PZLys	Poly(ε-carbobenzoxy L-lysine)
S	Periodicity of cholesteric LC
SAXD	Small-angle X-ray diffraction
SAXS	Small-angle X-ray scattering
SEM	Scanning electron microscopy
SFM	Scanning force microscopy
TCE	Trichloroethylene
TEM	Transmission electron microscopy
TFA	Trifluoroacetic acid
THF	Tetrahydrofuran

1 Introduction

Over the past few decades, increasing attention has been paid to synthetic polypeptide materials, including their syntheses, properties, and applications [1–14]. Polypeptides are derived from amino acids and their derivates. The continuing interest in polypeptides is mainly stimulated by their close relationship with proteins. Polypeptides can be used as a model system for protein research. Learning from natural proteins, polypeptides with diverse structures and functionalities have been widely synthesized and studied. The biorelated applications of the polypeptides and their assemblies are active topics of current research.

Polypeptides can be synthesized through biological and chemical methods [15]. In biological strategies, pure polypeptides with exact molecular weights and identical monomer sequences can be obtained [16–18]. Chemical techniques can be applied to prepare polypeptides with high molecular weights and are also advantageous for preparing polypeptide–polymer conjugates [19–25]. The most applied chemical method for polypeptide synthesis is the *N*-carboxyanhydride (NCA) route, which was first proposed by Leuchs about 100 years ago [26]. The synthesis of high molecular weight polypeptides and diverse polypeptide–polymer conjugates makes the research on polypeptides an active topic.

One of the unique properties of polypeptides is that they can adopt various conformations such as intramolecularly H-bonded α-helix, intermolecularly H-bonded extended β-sheet, and flexible random coil [5, 27]. For high molecular weight polypeptides, the α-helix conformation is a predominate structure.

Polypeptides with low molecular weights usually adopt the β-sheet conformation. When polypeptides are dissolved in denaturant solvents, the random coil conformation can be observed [28, 29].

The ordered structures assembled from polypeptide homopolymers and copolymers in both bulk and solution have attracted a great deal of attention over the past few decades and could continue to be an active theme in the future [30–38]. In solution, both the α-helix and β-sheet conformations of polypeptides facilitate the formation of ordered structures in liquid crystals (LCs), gels, and micelles during the assembly process. Usually, LC structures are assembled from polypeptide homopolymers in concentrated solutions [39–41]. In solutions with moderate concentrations, gels are usually formed by both polypeptide homopolymers and copolymers [42–44]. In dilute solutions, polypeptide copolymers are able to self-assemble into diverse micelle structures with a solvophilic shell, while the solvophobic polypeptide chains are packed in an ordered manner in the micelle core [45–47].

The ordering of polypeptide chains, typically for α-helix conformation, is similar in the structures of LCs, gels, and micelles. In LCs, polypeptide homopolymers are usually packed in a side-by-side manner to form a highly ordered arrangement in the form of nematic and cholesteric phases [39, 40]. For polypeptide homopolymers with identical chain length (polydispersity index, PDI = 1.0) or polydisperse polypeptides end-capped with a bulky group, a smectic LC phase can be observed [48, 49]. In homopolymer gel structures, larger dislocation of side-by-side packing of polypeptide helices is essential to form fiber-like structures as well as physical crosslinkers [42, 50–52]. For block copolymer gels, because of the existence of flexible chains, a smectic-like packing manner of polypeptide helices is adopted, in which the long axis of polypeptide helices is perpendicular to the long axis of gel fiber, and the flexible chains are spread out into the surroundings [44, 48, 53, 54]. Polypeptide-based copolymer micelles self-assembled in dilute solutions can preserve the ordered packing of polypeptides in the aggregates of cylinders, vesicles, and complex hierarchical structures. The ordering nature within the domain endows the polypeptide micelles with unique properties compared with conventional coil–coil type copolymer micelles, e.g., high stability and diverse morphologies [55–59]. For the polypeptides with β-sheet conformation, ordered structures can be achieved by parallel or antiparallel packing of polypeptide chains, which can be found in polypeptide gels and micelles [36, 54, 60]. When the α-helix or β-sheet conformation transforms to a random coil conformation, the ordering feature of polypeptides in these structures is destroyed and a subsequent variation in structure and morphology can be observed [61–63].

The research on polypeptides and their assembly behaviors is important and beneficial for several areas. First, polypeptides can be used as a model polymer with various chain rigidities. Polypeptides can adopt conformations of α-helix, β-sheet and random coil, which can transform into each other under controlled conditions. The α-helix to random coil transition in solutions is especially interesting. Thus, polypeptides can serve as an ideal model for investigating the influence of polymer rigidity on the assembly behavior of polymers. Second, the synthetic polypeptides

can be regarded as a simple model for proteins. Both α-helix and β-sheet conformations are basic secondary structures of proteins. The studies on ordered structures of the polypeptides, especially in hierarchical structures, can contribute to the prediction of the tertiary structures of proteins. Third, due to their biocompatibility and biodegradability, polypeptides and their assemblies are promising candidates as biorelated materials for use in, for example, drug delivery and tissue engineering scaffolds. Overall, the research on polypeptides and their ordered structures can enrich our knowledge of polymer science and also provide useful information for preparing advanced materials for medical and biotechnological applications.

In this review, we summarize the features of polypeptide ordered structures in LCs, gels and micelles and outline recent advances in this field. The article is divided into four main parts. The first part reviews the ordering of polypeptide homopolymers in LC structures. Polypeptides with rigid α-helix conformation can form LCs in concentrated organic solutions. Common aspects of the LC structures are briefly described. Recent advances, such as the conformation-induced cholesteric LC chirality transitions, the discovery of smectic phase, and the reentrant isotropic transitions, are the main content of the section. In the second part, ordering of polypeptide chains in gels is discussed. The structure of homopolymer gels is compared with homopolymer LCs and studies on copolymer gels are featured in detail. Samples formed in both organic and aqueous solutions are referred to. The ordering of polypeptides in self-assembled micelles in dilute solution is summarized in the third section. The ordering structures can be found in self-assemblies of cylinders and vesicles. The ordered packing tendency makes polypeptide copolymers an important candidate for producing hierarchical aggregates. Lastly, conclusions and outlook are presented.

2 LC Structures of Polypeptide Homopolymers

Polypeptides adopt α-helix conformation when they are dissolved in organic solvents such as *N,N′*-dimethylformamide (DMF), $CHCl_3$, and benzene. When the concentration is relatively high, LC structures are usually formed by the side-by-side ordered packing of rigid polypeptide chains. The ordering characteristics of polypeptides was first observed from the LC structure [39, 49, 64–72]. The formation of polypeptide LCs requires two crucial characteristics, rigidity of the polymer chain and ordering of the rod chains. Thus, only the α-helix polypeptide supports the LC structures. The helix-to-coil transition of polypeptide chains can destroy the LC ordering. In this section, typical LC structures and the arrangement of polypeptide chains in the LCs are discussed.

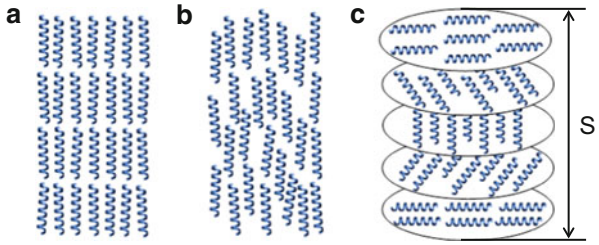

Fig. 1 Classification of polypeptide LCs: (**a**) smectic, (**b**) nematic, and (**c**) cholesteric phases. *S* indicates the periodicity of cholesteric LC

2.1 Typical LC Structures

LCs of polypeptide homopolymers were first described in the 1950s by Elliott and Ambrose, who observed a birefringent solution phase of poly(γ-benzyl L-glutamate)/chloroform (PBLG/$CHCl_3$) mixtures [71]. As shown in Fig. 1, polypeptides are able to form classical LCs with smectic, nematic and cholesteric phases. Smectic LC (Fig. 1a) shows the highest degree of order among the three phases, and is mainly found for polypeptides with identical degrees of polymerization (DPs). In the smectic phase, polypeptide chains are positionally ordered along one direction, forming well-defined layers that can slide over one another. In the nematic phase (Fig. 1b), polypeptide chains have no positional order and self-align to have long-range directional order with their long axes roughly parallel. Aligned nematics have the optical properties of uniaxial crystals, which makes them useful in LC displays. The most common polypeptide LC structure is the cholesteric phase (Fig. 1c). This phase exhibits a twisting of the molecules perpendicular to the director, with the molecular axis parallel to the director. The polypeptide molecules rotate by a small constant angle from one layer to the next. The cholesteric LCs show a unique property in that they reflect circularly polarized light when it enters along the helical axis and elliptically polarized light if it comes in obliquely. When the rotated angle of neighboring layers is zero, the cholesteric LC structure transforms to nematic phase. Therefore, in some cases, the cholesteric LC structure is classified as a chiral nematic phase.

2.2 Nematic and Cholesteric LC Structures

The most prominent characteristic of cholesteric LC is a set of equally spaced parallel lines (bright and dark lines) somewhat reminiscent of a fingerprint when observed by polarizing optical micrograph (POM). The distance between the alternating bright and dark lines is called the periodicity *S*, which is equal to half the pitch of the torsion of cholesteric LC. Such experimental results are explained by a helicoidal structure, as shown in Fig. 1c.

The periodicity *S* of polypeptide LCs is found to be dependent on the temperature, polymer concentration, solvent nature, molecular weight, etc. [40, 73–75].

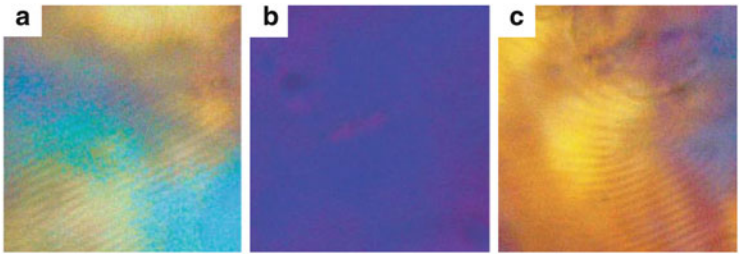

Fig. 2 POM observations of a concentrated PClBLA solution (25 wt%) in TCE. The birefringent cholesteric texture changes its sign from (**a**) left (90°C) to (**c**) right (102°C) with increasing temperature. (**b**) The cholesteric pitch diverges in the transition region (97°C). The screw sense of the polypeptide backbone transforms from right to left, accordingly. Reprinted with permission from [76]. Copyright 2005 Wiley-VCH

For example, for the system of PBLG/m-cresol LCs, in the temperature range of 30–60°C, right-handed cholesteric LCs are observed and the periodicity *S* increases with increasing temperature [74]. At 60°C, the cholesteric character disappears and nematic LCs are formed. Above this temperature, left-handed cholesteric structures appear and the periodicity *S* decreases with increasing temperature. Regarding the dependence on the nature of the solvent, results from the PBLG LCs formed in dioxane-dichloroethane mixed solvent showed that the chirality of the LC transformed from right-handed to left-handed with increasing volume fraction of dichloroethane [75]. For such phenomenon, the dielectric constant of the solvents is believed to be one of the important influencing factors. Usually, a solvent with lower dielectric constant supports a right-handed cholesteric structure.

In addition, the chirality of polypeptide backbones was found to have a remarkable influence on the handedness of LC structures. For example, Abe et al. investigated the LC structure of poly(β-*p*-chlorobenzyl L-aspartate)/trichloroethylene (PClBLA/TCE) systems [76]. They found that the chirality of the LCs is opposite to the screw sense of the polypeptide backbone. At room temperature, PClBLA takes the right-handed α-helical conformation, while the chirality of the LC is left-handed. Discrete conformation change of the polypeptide from right-handed to left-handed α-helical takes place between 80 and 100°C. Accordingly, the LC structures change from left-handed to right-handed, separated by the nematic phase. Figure 2 shows the POM images of LC structures that changed from left cholesteric (90°C) to nematic (97°C) and then to right cholesteric (102°C) with increasing temperature.

In another work on poly(β-phenethyl L-aspartate)/trichloroethylene/dichloroacetic acid (PPLA/TCE/DCA) systems, they found a more complex LC phenomenon [77]. With increasing the solution temperature, the screw sense of the polypeptide backbone changed from left-handed to right-handed and then to left-handed (L–R–L). The primary reason responsible for such a helix–helix transition resides in a small free-energy difference in the conformational states of the flanking side chain of the opposite handedness [78]. Simultaneously with the helix–helix transition,

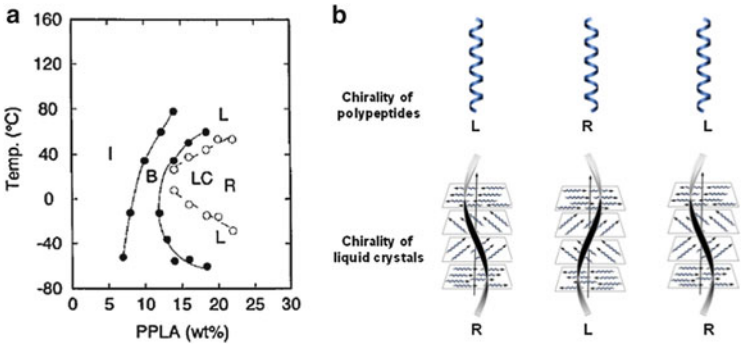

Fig. 3 (**a**) Phase diagrams for a ternary solution of PPLA in TFA/$CHCl_3$ (3/97 w/w). *Solid lines* indicate phase boundaries between liquid crystalline (*LC*) and isotropic (*I*) states and *dashed lines* those between right- and left-handed α-helical states; *B* biphasic region. (**b**) PPLA conformation-induced the transition of LC handedness. Reprinted with permission from [77]. Copyright 1997 Wiley-VCH

the handedness of LCs gradually changes from right to left and then to right (R–L–R). Thus, the temperature dependence of the LC structures can be divided into three characteristic regions: I ($T < 25°C$), II ($25°C < T < 89°C$) and III ($T > 89°C$), each of which is separated by the nematic phase. The cholesteric sense inversion at the boundary between regions I and II, as well as between II and III, is triggered by the reversal of the screw sense of the α-helical backbone. When DCA is eliminated from the system, the transitions shown in the lower part of Fig. 3a tend to be suppressed and a result similar to that presented in Fig. 2 from PClBLA/TCE solution can be obtained.

2.3 Smectic LCs

Smectic ordering is common in low molecular weight LC compounds and has also been observed for rodlike tobacco mosaic virus in colloidal solutions [49, 64]. However, the smectic LC phase in solution is rarely observed for polypeptide homopolymers due to the polydisperse nature of chemically synthetic polypeptide. Tirrell's group reported for the first time the formation of smectic LC structures from monodisperse polypeptides derived from PBLG (DP = 76, counter length 114 Å), which was synthesized via recombinant DNA technology [49]. The LCs of modified PBLG were obtained in mixtures of $CHCl_3$ (97%, v/v) and trifluoroacetic acid (TFA; 3%, v/v). The addition of TFA inhibits aggregation of PBLG in concentrated solutions while the low concentration does not destroy the rigidity of polymer chains. Figure 4a shows a POM image of a ~35 wt% solution of PBLG in $CHCl_3$/TFA. The solution is iridescent with a fan-like texture suggestive of smectic order. The solution-cast films maintained their LC order after solvent

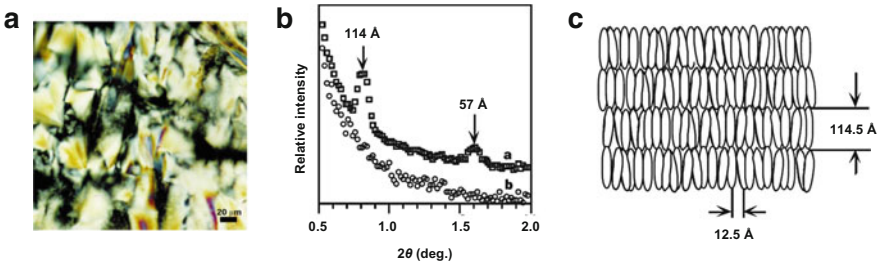

Fig. 4 (**a**) POM image of PBLG in $CHCl_3$/TFA. (**b**) Densitometer scans of the SAXD patterns of films prepared from solutions of monodisperse PBLG (*curve a*) and polydisperse PBLG (*curve b*). (**c**) Smectic structure of PBLG, showing the origin of the 12.5 Å and 114.5 Å reflections. Reprinted from [49], by permission from Macmillan Publishers Ltd: Nature, copyright (1997)

evaporation. The densitometer scan of the SAXD pattern of the film (Fig. 4b, curve a) shows a well-defined maximum at a spacing of 114.5 ± 1.4 Å, as well as the corresponding second-order reflection at 57.0 ± 0.3 Å. The coincidence of the helix length and the observed layer spacing strongly suggests smectic-like ordering in the cast solid film. In contrast, a solid film of polydisperse PBLG with comparable molecular weight (DP ≈ 98, PDI = 1.2) yields no small-angle reflections in a similar diffraction experiment (Fig. 4b, curve b). Shown in Fig. 4c is the illustration for the smectic LC structures. As can be seen, the helical rods arrange in layers of thickness 114.5 Å, and the distance between two PBLG rods is 12.5 Å, which corresponds to the diameter of PBLG rods.

The polydispersity of polymer is the main reason for the lack of a smectic LC phase of chemically synthetic polypeptides. However, when a compact and bulky group is capped on polypeptide ends, the situation can be rather different. During self-assembly in concentrated solutions, such modified polypeptides can self-assemble into a smectic LC phase [48, 79]. For example, Winnik et al. found that dendron-helical PBLG (DHP; Fig. 5a) copolymers can form smectic phases in $CHCl_3$ [48]. The dendritic block prevents the DHP copolymers from aligning into a nematic phase. As shown in Fig. 5b, the concentrated solution (>40 wt%) of the DHP copolymers in THF shows a birefringent texture under the POM observation. SAXS experiments on the dried solid from the concentrated THF solution show two diffraction peaks at 7.2 and 3.3 nm, which suggests that the DHP exhibits smectic-like order in concentrated solution. The proposed two-dimensional layer structure of DHP that results from an antiparallel stacking of DHP is presented in the inset of Fig. 5b. The result suggests that smectic ordering of the DHP copolymers in solution is feasible with a dendritic molecule as a non-random coil block, even though the PBLG block is polydisperse in chain length. However, it should be noted that due to the polydispersity of PBLG blocks and the flexible nature of the peripheral alkyl chains of the dendron block, the LC phase of DHP is not well ordered and thus it is proper to call the LC structure a "smectic-like" phase.

The success in constructing highly ordered smectic phase in solution by using modified polydisperse polypeptide homopolymers rather than monodisperse

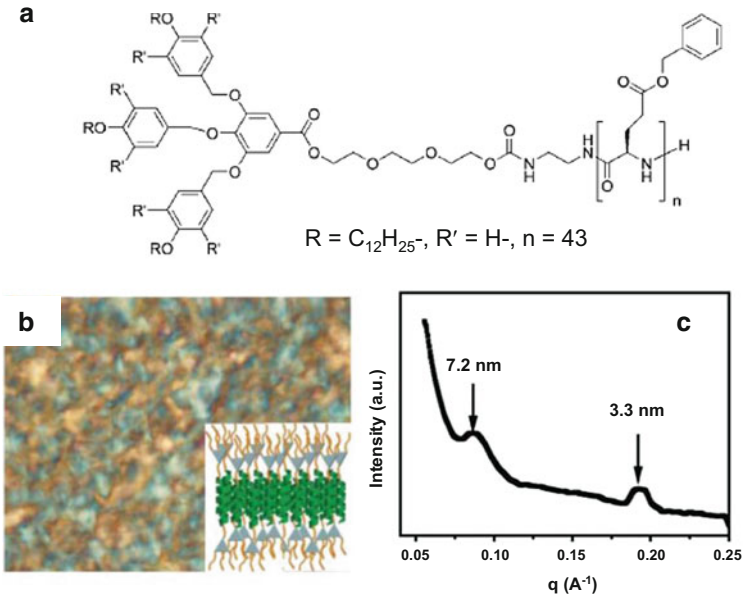

Fig. 5 (**a**) Molecular structure of dendron-helical polypeptide (DHP) copolymers. (**b**) Optical birefringent texture of THF solution of DHP (40 wt%) and proposed layered structures of LC state (*inset*). (**c**) SAXS profile of dried solid of THF solution. Reproduced from [48] with permission of The Royal Society of Chemistry

samples is significantly valuable for the preparation of well-defined supramolecular structures. From smectic PBLG LCs, highly ordered ultrathin PBLG films with controlled layer spacing and thickness can be prepared. When the rods are oriented perpendicular to the substrate, they can be used as nonlinear optical and piezoelectric materials [49, 64]. When the rods in the films are organized parallel to the substrate, the mono- or multilayer films are useful in creating patterned arrays for use in sensor technology. In addition, the LCs can be further functionalized through functionalizing the tethered bulky groups or polymer chains. The findings on the smectic LC structure from modified polydisperse PBLG thus not only promote understanding of the fundamental physics of rodlike polymers, but also have substantial impact for the application of rodlike polymers in a variety of technologies.

2.4 Reentrant Isotropic Transition of Polypeptide LCs

Polymer chains with fully rigid conformation are rare in nature. Usually, the nematogenic chain molecules are able to adopt a variety of conformations, some more extended and rodlike than others. Occurrence of liquid crystallite in such

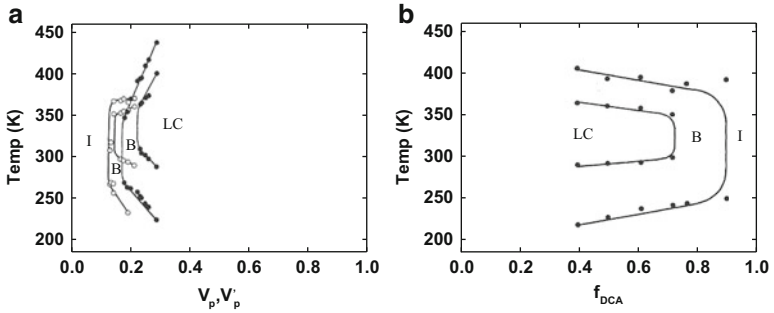

Fig. 6 (**a**) Phase diagram for PBLG/DCA/EDC ternary system. *Open circles* indicate the values obtained for PBLG (M_v = 130,000) dissolved in DCA/EDC (85.3/14.7 w/w). *Solid circles* are those for PBLG (M_v = 62,000) dissolved in DCA/EDC (80/20 w/w). (**b**) Phase boundary curves of PBLG/DCA/EDC solutions as functions of acid composition at a given polymer volume fraction of 0.25, where f_{DCA} (mole fraction) = DCA/(DCA + EDC). *I* Isotropic phase, *B* biphasic region, *LC* liquid crystalline phase. Reprinted with permission from [80]. Copyright 1997 Elsevier

systems must invariably be accompanied by selective reorganization favoring more extended chain conformations. The intramolecular conformational change can, therefore, be coupled with the isotropic–anisotropic transition and be accelerated by the intermolecular order. Such an effect is termed "conformational ordering" and pertains to semi-rigid chains in general.

An example of conformational ordering is the reentrant isotropic phase transition in polypeptide LCs. In the presence of a denaturant acid, the polypeptide molecules tend to adopt a random coil state by lowering the temperature [80–82]. An anisotropic–isotropic transition(reentrant transition) occurs at low temperature because the coil chain is unable to support the LC ordering. Shown in Fig. 6a is a typical phase diagram of a PBLG/DCA/dichloroethane (PBLG/DCA/EDC) system in which PBLG samples have relative molecular weights (M_r) of 130,000 and 62,000 [80]. Two anisotropic–isotropic transitions occur at high and low temperatures, with the latter a result of the intramolecular conformation transformation from helix to coil. An acid-induced LC to isotropic transition was also observed. The result is replotted in Fig. 6b. With increasing acid content, the LC phase tends to be destabilized along both the high- and low-temperature boundaries. In the range of high acid concentrations, no LC phase could be observed at any temperature due to the coiled molecular conformations being unable to sustain the anisotropic ordering. The helix structures tend to remain more stable in the LC state than in the isotropic phase due to the conformational ordering effect exerted by the environment.

Regarding the theoretical considerations for the possibilities of a reentrant isotropic phase in the polypeptide LC, Lin et al. proposed a theory based on the Flory–Matheson lattice model in which the free energy change for the helix–coil transition has been incorporated into the lattice scheme [80]. Some assumptions were also adopted. First, the molecular conformation in the isotropic phase was considered to be temperature-dependent and follow a modified Zimm–Bragg notion

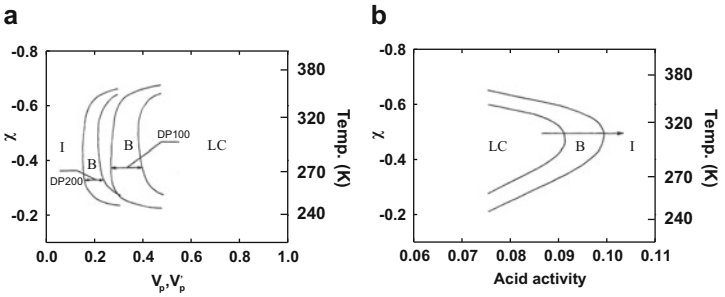

Fig. 7 (**a**) Phase diagrams calculated for DP = 100 and 200. (**b**) Plot of solvent–polymer interaction parameter (χ) values and phase transition temperatures versus acid activity at a given polymer volume fraction of 0.45. *I* Isotropic phase, *B* biphasic region, *LC* liquid crystalline phase. Reprinted with permission from [80]. Copyright 1997 Elsevier

for the helix–coil transition, in which the acid effect has been taken into account. Second, the solvent–polymer interaction parameter (χ) was considered to be negative in the whole temperature range and was regarded as an inverse measure of temperature.

Figure 7a shows a typical calculated phase diagram for polypeptides in denaturant solvents. Two samples of DP = 100 and DP = 200 are considered. Taking the curve for DP = 100 as an example, on the left-hand side of the diagram (low polymer volume fraction, v_p) all solutions are isotropic. Within the intermediate χ value or temperature range, a single anisotropic phase forms when the polymer concentration becomes higher. The transition from the isotropic to the anisotropic phase is bridged by a biphasic chimney-like region. As the temperature goes down, or equivalently χ turns positive, v_p and v_p' tend to be higher, and eventually no anisotropic phase can be formed. In other words, with a decrease in temperature, an anisotropic-to-isotropic reentrant transition caused by the intramolecular helix–coil transformation is predicted. In this reentrant isotropic region, the rigid helix anisotropic phase is in equilibrium with an isotropic solution comprising flexible chain molecules. At higher temperatures, a gradual blending of the chimney region towards a higher concentration region is demonstrated. Such a blending is related to the enhanced chain flexibility in the isotropic phase caused by the thermal energy at elevated temperatures, as normally observed in real polymer systems. These results reproduced well the experimental observations shown in Fig. 6a.

The effect of acid activity on the reentrant isotropic phase was also examined. Figure 7b shows the theoretical results for both high- and low-temperature anisotropic–isotropic transition temperatures as functions of acid activity at a given polymer concentration. As can be seen, with increasing acid content, the LC phase tends to be destabilized along both the high- and low-temperature boundaries and lower temperature reentrant isotropic transition tends to take place at higher temperatures. In the range of high acid concentration, no LC phase could be detected at any temperature due to the coiled molecular conformations being unable to sustain the anisotropic ordering. These predictions are also in line with the experiments shown in Fig. 6b.

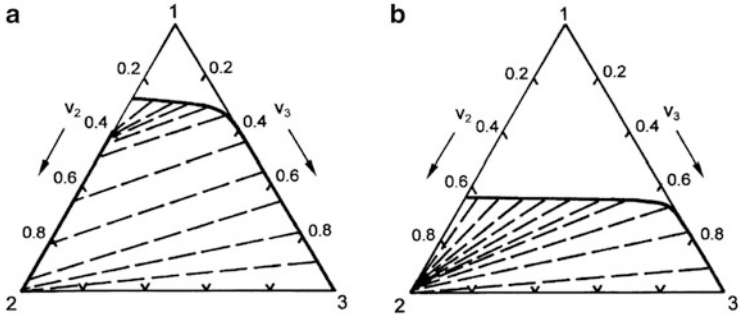

Fig. 8 Phase diagrams calculated for the ternary systems at (**a**) 300 K and (**b**) 245 K; v_2 and v_3 are the volume fraction of polypeptide and coil polymer, respectively. Reprinted with permission from [83]. Copyright 2003 American Chemical Society

Lin et al. further extended the theoretical considerations from binary systems to ternary systems involving polypeptide chain and a randomly coiled polymer [83]. Two polymers are predicted to be miscible in isotropic phase. However, the flexible chains are severely excluded from conjugated anisotropic phases (see Fig. 8a). If denaturing component is present in the ternary system, the polypeptide can undergo helix–coil transition as the temperature decreases. Such a reduction in the backbone rigidity should enlarge the miscible isotropic phase, as shown in Fig. 8b. A further decrease in temperature could result in entire elimination of the anisotropic phase (reentrant isotropic phase) due to the random coil polypeptide structure being unable to support the anisotropic ordering. On the other hand, increasing temperature results in diminishing of the anisotropic–isotropic biphasic area. At higher temperatures, the polypeptide chains become flexible. As a result, the LC phase diminishes because of the flexible chains being unable to support the anisotropic ordering.

The lattice model, as put forth by Flory [84, 85], has been proved successful in the treatments of the liquid crystallinity in polymeric systems, despite its artificiality. In our series of work, the lattice model has been extended to the treatment of biopolypeptide systems. The relationship between the polypeptide ordering nature and the LC phase structure is well established. Recently, by taking advantage of the lattice model, we formulated a lattice theory of polypeptide-based diblock copolymer in solution [86]. The polypeptide-based diblock copolymer exhibits lyotropic phases with lamellar, cylindrical, and spherical structures when the copolymer concentration is above a critical value. The tendency of the rodlike block (polypeptide block) to form orientational order plays an important role in the formation of lyotropic phases. This theory is applicable for examining the ordering nature of polypeptide blocks in polypeptide block copolymer solutions. More work on polypeptide ordering and microstructure based on the Flory lattice model is expected.

3 Ordering of Polypeptides in Gel Structures

Gels are soft materials comprising a liquid-like phase and a solid network, the latter preventing the bulk flow of the liquids. They have potential in diverse applications for tissue engineering, nanoscale electronics, etc. Polymer gels are usually formed in a moderately concentrated solution, in which physical or chemical crosslinks are necessary. Both polypeptide homopolymers and copolymers can assemble into gel structures. Similar to that in LCs, the ordering of polypeptide chains takes important responsibility for the gelation behavior. In addition to the α-helix conformation, the β-sheet conformation also supports the formation of polypeptide gels. In this section, the ordering of polypeptides in gel structures is discussed. The content is organized into three subsections. The first section describes the organic gels formed by polypeptide homopolymers, the second polypeptide block copolymer gels in organic solvents, and the third hydrogels formed by polypeptide block copolymers in aqueous solutions.

3.1 Polypeptide Homopolymer Gels in Organic Solvents

Polypeptide homopolymers (typically PBLG) with rigid α-helix conformation can form LC structures at a high concentration and temperature. When the solution is cooled, a transparent, mechanically self-supporting gel is always observed [42, 87–91]. The gel formation was found to be concentration and temperature dependent and completely reversible. It is well known that the physical or chemical crosslinks are necessary for polymer gels. Flexible polymers can easily form crosslinking domains with crystalline or semicrystalline structures. However, for rigid polypeptide chains, it is less clear how the rodlike polypeptides participate extensively in intermolecular crosslinks.

There are various approaches to explain this effect but a common aspect is that rigid polypeptide chains aggregate into nanofibers and the interfiber crosslinking results in the formation of networks. Figure 9a shows a TEM photograph of the PBLG gels from DMF (concentration 1 wt%) [42]. Random networks were observed to be formed by branching and rejoining of different strands. The strands are of diameters ranging from tens to hundreds nanometers and are composed of bundles of aligned rods (rod diameter ~2 nm, corresponding to the diameter of PBLG helix). The benzene ring interaction or stack, as well as the dislocated side-by-side packing tendency of PBLG rods, is responsible for the formation of such strands. Figure 9b shows a scheme for the polypeptide gel structure. As can be seen, physical crosslinks are formed by the branching and rejoining of different sheaf-like aggregates, which stabilize the gel structures in solution.

Usually, gels are physically crosslinked and the ordered structures cannot be preserved under heating or other treatments because of the breakage of the physical crosslinks. However, when the gels are chemically crosslinked, the shape and inner

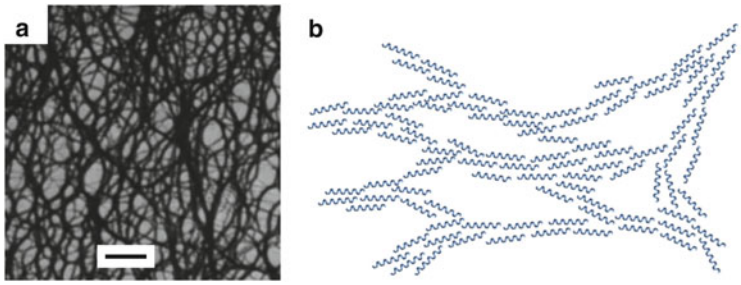

Fig. 9 (**a**) TEM photograph of a PBLG-DMF gel (dry state, scale bar = 1 μm). (**b**) Model of networks formed by aggregation of rigid polymers. Reprinted by permission from Macmillan Publishers Ltd: Nature, [42], copyright (1981)

structure of the gels can be recovered by reversing the solution conditions. An example is crosslinked "LC gel." The LC polypeptide gels are usually prepared by crosslinking the LC polypeptides (typically using diamines) and subsequently lowering the solution temperature [92–94]. Very recently, Inomata et al. reported a preparation of uniaxially oriented PBLG LC gels by crosslinking the lyotropic LC PBLG through pentaethylenehexamine in a magnetic field. Meanwhile, the PBLG was converted to PHEG by side chain aminolysis [94]. The obtained PHEG gel retains the LC structure when immersed in ethylene glycol, which is an α-helix-supporting solvent. By the addition of water into the immersion solvent, conformational transition of PHEG from α-helix to random coil occurs and the optical anisotropy of the gel disappears. With this helix-to-coil transition of PHEG, the gel is swollen in the direction perpendicular to the orientational axis of PHEG and is shrunk in the parallel direction. Such a reverse gel shape transition from cylindrical to isotropic with the change of the solvent from helix-supporting ethylene glycol to coil-supporting water is shown in Fig. 10. The original cylindrical shape in the LC state changes to the more isotropic shape as a result of the helix-to-coil transition of PHEG. Because the gel is crosslinked, not only the position but also the orientational order of the rodlike polypeptide chains is fixed. This anisotropic feature characteristic of polypeptide gels may be useful in shape-memory applications, in contrast to conventional stimuli-sensitive polymer gels that are in the disordered isotropic state.

3.2 Ordering of Polypeptides in Copolymer Organogels

Polypeptide copolymers can assemble into gels in organic solvent through ordered packing of polypeptide blocks with conformations of both α-helix and β-sheet [44, 48, 53, 54, 95–100]. For copolymers with α-helix polypeptides, the side-by-side packing of the polypeptide rods in a smectic fashion has been commonly observed. For the copolymers with β-sheet polypeptides, the strong intermolecular

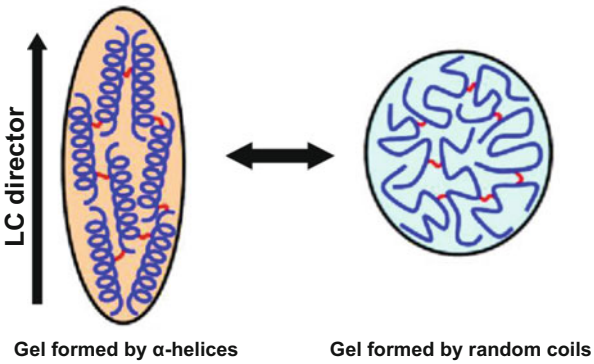

Fig. 10 Illustration of the helix-to-coil transition, anisotropic-to-isotropic transition, and shape change of the uniaxial PHEG gel. Reprinted with permission from [94]. Copyright 2012 American Chemical Society

attractions are responsible for the formation of stable gels. Due to the good solubility of polypeptide in diverse solvents, organogels can be easily prepared at the proper concentration and temperature. In the following section, we discuss the formation of organic gels from polypeptide block copolymers with both α-helix and β-sheet conformations.

3.2.1 Organic Gels from Polypeptide Copolymer with α-Helix Conformation

Polypeptides with α-helix conformation prefer to take ordered packing in solutions and thus induce the formation of LCs and gels. Similar to LC structures formed by bulky group-capped polypeptide homopolymers, as described in the Sect. 2.3, the smectic-like rather than nematic ordering of polypeptide rods is preferred for polypeptide block copolymers. In the polypeptide copolymer gels, the long axis of the polypeptide rods is usually perpendicular to the long axis of gel fiber. Winnik et al. reported, for the first time, thermoreversible gelation of polypeptide block copolymers in organic solvent [44]. In their work, poly(ferrocenylsilane)-*b*-PBLG (PFS-*b*-PBLG) block copolymers (Fig. 11a) were first dissolved in hot toluene. Upon cooling to ambient temperature, optically transparent gels were formed (Fig. 11b). Fibrous nanoribbons can be observed in the AFM image shown in Fig. 11c. For these gels, the strong dipolar interactions between the PBLG helices are proposed to stabilize the stacked structure, where the PFS blocks protrude outside of the ribbon into the toluene-rich environment, thereby preventing aggregation of the nanoribbons. The gel structure is illustrated in Fig. 11d. As can be seen, PBLG rods assembled in one-dimensional antiparallel stacking of the building blocks in a monolayer fashion, and the flexible PFS blocks extended off the fibers.

In a recent work, Mezzenga et al. synthesized PBLG-*b*-PDMS-*b*-PBLG triblock copolymers with DP of PBLG blocks from 24 to 120. For these block copolymers, the conformation of the PBLG blocks is mainly α-helix. Thermoreversible gels were prepared in toluene [63]. The gel structure is illustrated in Fig. 12a and shows that PBLG rods are confined within the core of the nanofibrils, whereas the soluble

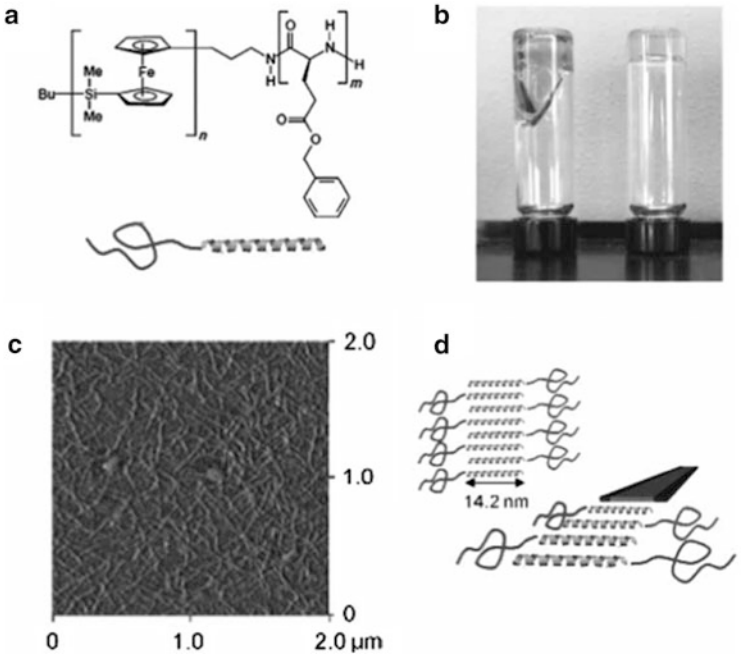

Fig. 11 (**a**) Structure of PFS-*b*-PBLG block copolymer. (**b**) Optical photograph of inverted vials containing a toluene-swollen gel. (**c**) AFM image of PFS-*b*-PBLG gel. (**d**) Scheme of the nanoribbon formed in the network structure of the gel. Reprinted with permission from [44]. Copyright 2005 Wiley-VCH

PDMS coils remain exposed to the toluene. They found that the thickness of the nanofibrils changes little with the DP of PBLG blocks. As shown in Fig. 12b, for the sample with the shortest PBLG block (DP = 24), PBLG rods assembled into a bilayer morphology with 7 nm thickness. Increasing the DP to 43, a monolayer morphology with 6–8 nm thickness is observed (Fig. 12c). Interestingly, for the sample with the longest PBLG block (DP = 120), PBLG rods are packed with a folded manner to produce 9-nm thick fibrils (Fig. 12d).

3.2.2 Organic Gels from Polypeptide Copolymer with β-Sheet Conformation

Strong interchain attractions between polypeptides with β-sheet conformation enable polypeptide chains to pack in an orderly manner, which facilities the formation of gels. Furthermore, these polypeptide gels are more stable because the interchain attractions between β-sheets are much stronger than those between helix–helix pairs. Schlaad and coworkers have investigated the effects of the secondary structure of polypeptides on the gelation of polypeptide-based organogelators in THF [36]. Three poly(ethylene oxide)-*b*-poly(ε-carbobenzoxy L-lysine)

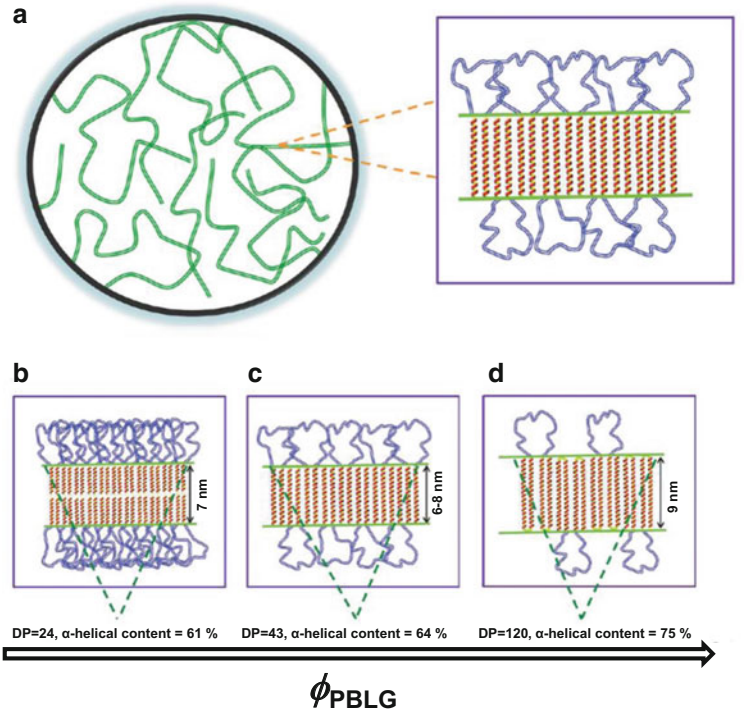

Fig. 12 (**a**) Self-assembly of the PBLG rods during the nanofibril formation for the PBLG-*b*-PDMS-*b*-PBLG triblock copolymers. (**b**–**d**) Changes in thickness due to the increase in the degree of polymerization of the PBLG block: (**b**) DP = 24, a head-to-head bilayer morphology of the α-helical rods; (**c**) DP = 43, a monolayer morphology; and (**d**) DP = 120, a head-to-head packing of folded α-helical rods. Reprinted with permission from [63]. Copyright 2012 American Chemical Society

(PEO-*b*-PZLys) block copolymers (samples 1, 2 and 3) with various polypeptide conformations were synthesized. All the polypeptide blocks consisted of 18 ZLys peptide segments with D and L configurations of predefined stereosequences. In sample 1, D and L configuration peptide units are randomly polymerized (L_{10}-*co*-D_8) and the polypeptide conformation is random coil. In sample 2, D and L configuration peptide units link in a manner similar to that of a triblock copolymer ($L_7D_4L_7$) and the polypeptide conformation is β-sheet. In sample 3, all the peptide segments are in the L configuration (L_{18}) and thus the polypeptide adopts α-helix conformation. From the time-dependent evolution of the dynamic viscosity of THF solutions of the samples (shown in Fig. 13a), it was found that the tendency for gelation in THF increases in the order of the polypeptide conformation of random coil < α-helix < β-sheet. For example, at the concentration of 20 g/L, samples 1 and 3 are liquids and sample 2 is a gel (Fig. 13b). From the set of SFM images shown in Fig. 13c–e, one can see that sample 1 formed spherical micelles (Fig. 13c) whereas

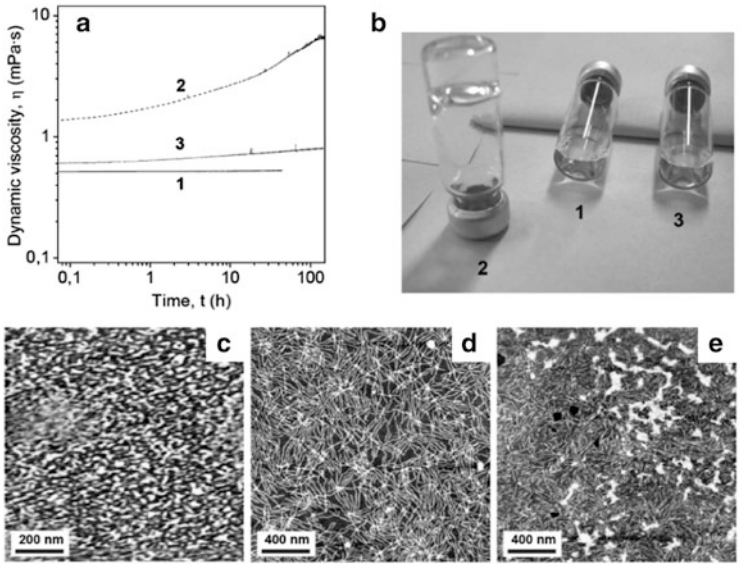

Fig. 13 (**a**) Time-dependent evolution of the dynamic viscosity of THF solutions of samples *1–3* (5 g/L) at room temperature. (**b**) Photographs of samples at 20 g/L in THF. (**c–e**) SFM height images of samples *1* (**c**), *2* (**d**), and *3* (**e**) at 20 g/L in THF. Reprinted with permission from [36]. Copyright 2011 American Chemical Society

nanofibrils formed for sample 2 and 3 (Fig. 13d, e). Evidently, the fibrils of the gelled sample 2 are considerably longer than those of the nongelled sample 3.

Organogels could potentially be used in fields of template synthesis and functional materials [101–104]. Stable organogels with controlled structure and functionality are thus highly desired to meet practical applications. The high stability of the polypeptide gels due to the ordered packing tendency of the polypeptide chains is a significant advantage. Meanwhile, polypeptide blocks are easily functionalized, which makes them promising candidates for preparation of organogels with diverse functions. Moreover, the variability of the chirality of the polypeptide backbone should bring additional opportunity to fabricate smart organogels. However, there are few works so far on the preparation of functional organogels with controlled structures. Further investigations are needed on the dependence of structure and functionality of organogels on polypeptide building blocks as well as on preparation strategies.

3.3 Hydrogels Formed by Polypeptide Block Copolymers

In recent years, hydrogels have obtained increasing attention because they have promising applications in biorelated areas, e.g., drug delivery, tissue engineering, etc. [2, 105–116]. Because hydrophobic polypeptide chains cannot be dissolved in

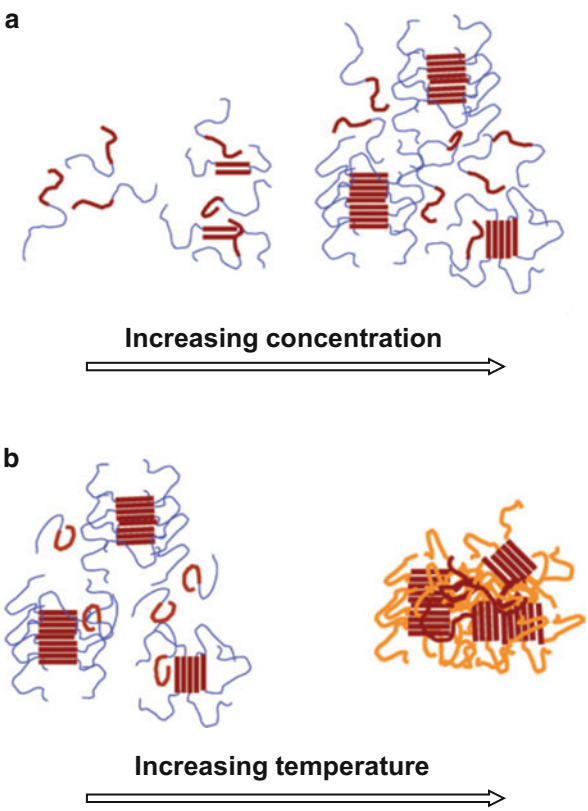

Fig. 14 (**a**) Conformational changes of PEG-*b*-L-PA in water as a function of polymer concentration. *Thick straight brown lines, thick flexible brown lines*, and *thin flexible blue lines* denote the β-sheet structure, random coil structure and flexible PEG, respectively. (**b**) Temperature-induced sol-to-gel transition of PEG-*b*-L-PA. As the temperature increases, PEG (*thin flexible blue lines*) is partially dehydrated (*thick flexible yellow lines*). Reproduced from [117] with permission of The Royal Society of Chemistry

water, it is difficult for the copolymers bearing high molecular weight hydrophobic polypeptide blocks to form hydrogels. On the other hand, hydrophilic polypeptides usually adopt a random coil conformation, which does not support the formation of gel containing ordered structures. As a result, polypeptide hydrogels are usually formed by copolymers consisting of low molecular weight polypeptides. This section discusses the formation of polypeptide copolymer hydrogels based on both β-sheet and α-helix polypeptide blocks.

3.3.1 Hydrogels Based on β-Sheet Polypeptide Copolymers

Jeong et al. studied the gelation behavior of poly(ethylene glycol)-*b*-poly(L-alanine) (PEG-*b*-L-PA) block copolymers in water [117, 118]. They suggested that the β-sheet structure of L-PA plays a critical role in developing a fibrous nanostructure as well as in the sol-to-gel transition of the copolymer solutions (Fig. 14). The conformation of L-PA in water is random coil at low concentrations. As the concentration increases, block copolymers start to aggregate and the conformation

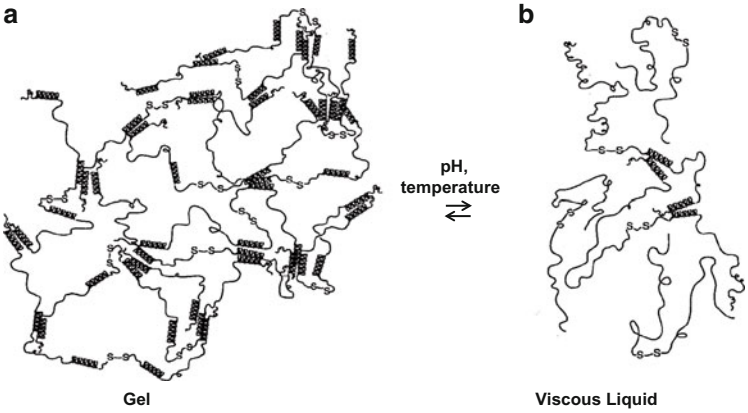

Fig. 15 Proposed physical gelation of monodisperse triblock artificial protein: (**a**) gel; (**b**) viscous liquid. From [119]. Reprinted with permission from AAAS

of L-PA transforms to β-sheet. Further increase of the polymer concentration results in nanofibrous rod formation through the packing of the β-sheet in a one-dimensional manner. Such a nanostructural growth can be stabilized by the hydrophilic PEG blocks (Fig. 14a). As the temperature increases, the PEG blocks are partially dehydrated and the sol-to-gel transition occurs by the further aggregation of preassembled PEG-*b*-L-PA aggregates at high concentrations of polymer (Fig. 14b). As a controlled experiment, they also studied the gelation behavior of PEG-*b*-DL-PA block copolymers in the same conditions. Poly(DL-alanine) (DL-PA) always takes random coil conformation. With increasing polymer concentration, the PEG-DL-PA cannot form specific nanostructures. Therefore, PEG-*b*-DL-PA shows a sol-to-gel transition at much higher concentrations and temperatures.

3.3.2 Hydrogels Based on α-Helix Polypeptide Copolymers

There are a few reports focused on hydrogels from block copolymers consisting of α-helix polypeptide segments. Tirrell et al. investigated the gelation of a multidomain ("triblock") artificial protein in which the interchain binding and solvent retention functions were engineered independently [119]. The authors describe a polypeptide consisting of 230 amino acids, 84 of which make up the helix repeat and 90 of which make up the alanylglycine-rich repeat. The helical motifs can form coiled-coil aggregates in near-neutral aqueous solutions, which trigger the formation of a three-dimensional polymer network, with the polyelectrolyte segments retaining solvent and preventing precipitation of the chains (Fig. 15a). Dissociation of the coiled-coil aggregates through increasing the pH or temperature causes dissolution of the gel (Fig. 15b). These hydrogels have potential

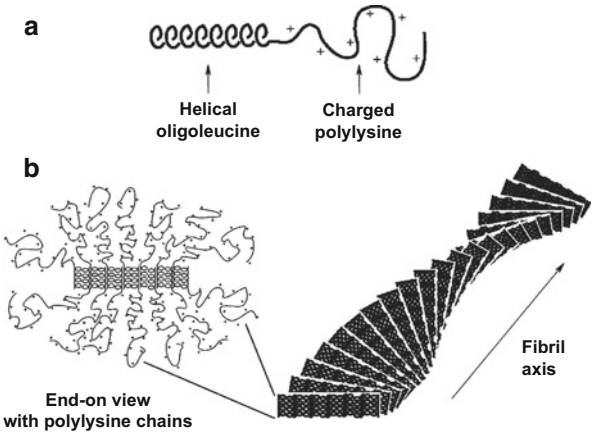

Fig. 16 (**a**) Representation of a block copolypeptide chain and (**b**) proposed packing of block copolypeptides into twisted fibrillar tapes. Polylysine chains were omitted from the fibril drawing for clarity. Reproduced from [105] with permission of The Royal Society of Chemistry

in bioengineering applications that require the encapsulation or controlled release of molecular and cellular species.

Studying the gelation behavior of poly(L-lysine)-*b*-poly(L-leucine) (PLL-*b*-PLeu) diblock copolypeptide, Deming et al. found that the self-assembly process of block copolymers is responsible for gelation and that the gel-forming ability increases with the length of water-soluble PLL chains [105, 107, 108]. The copolymer and gel structure models are presented in Fig. 16a, b. The longer PLL polyelectrolyte segments increase interchain repulsions so that the packing of PLeu hydrophobic helices, which appear to prefer to form flat two-dimensional sheets, must distort to minimize the overall energy of the system. The best way to do this, while maintaining favorable helix packing, is to twist the sheets into fibrillar tapes, where the tape width is determined by the degree of twist. In this model, the helices are still able to pack perpendicular to the fibril axis, but with a slight twist between planes of parallel packed helices.

From these examples, we conclude that both the α-helix and β-sheet conformations support the gelation of polypeptide homopolymers and copolymers. For homo-polypeptide organogels, the building polymers usually have large relative molecular weights (usually in the scale of 10^4–10^6), thus the strength of the gels can be quite good. However, for block copolymer gels, most polymers have low relative molecular weights (typically from hundreds to thousands), thus the mechanical property is poor, which inhibits their application. Improving the mechanical properties of polypeptide gels is one of the main tasks. Due to the strong intermolecular attractions, the polypeptide copolymers with β-sheet conformation have better gelation ability and strength. Thus, preparing copolymers with multiblocks of β-sheet polypeptide could be an efficient way to improve the gel strength. In addition, partially modifying high molecular weight polypeptide with hydrophilic segments, for example grafting hydrophilic side chains onto a hydrophobic polypeptide backbone, is also a promising approach for preparing stable hydrogels. However, related works are limited, especially for hydrogels. Studies of this topic are expected.

4 Ordering of Polypeptide Chains in Micelles

In dilute solutions, block copolymers can self-assemble into micelles with a core–shell structure, which have great potential applications in drug delivery systems, coatings, cosmetics, and nanoreactors [120–127]. In selective solvents, block copolymers consisting of solvophobic polypeptide segments, such as PBLG and PZLys, can self-assemble into diverse structures through ordering of polypeptide chains with the α-helix conformation. The helical polypeptide–solvophilic polymer conjugates are typical rod–coil copolymers. As compared with intensively investigated coil–coil block copolymers, the self-assembly behavior of rod–coil block copolymers is far from well studied. Polypeptide-based rod–coil block copolymers can be used as model copolymers for investigating the effect of ordered packing of the rods on the self-assembly behavior of block copolymers. Besides the α-helix conformation, ordered packing of β-sheet polypeptides is also observed in micelles. Graft copolymers are another important category of copolymers capable of forming aggregates. This section describes the ordering of polypeptide chains of block and graft copolymers as well as copolymer mixtures in assembly structures of cylindrical micelles, vesicles, and other complex structures.

4.1 Cylindrical Micelles Self-Assembled from Polypeptide Copolymers

The fiber-like structure of polypeptide block copolymers is essential in organogels that are formed by the side-by-side packing of polypeptide rods. Similarly, such side-by-side packing of polypeptide rods can also be found in cylindrical micelles self-assembled from polypeptide block copolymers. In both the fiber-like gels and cylindrical micelles, polypeptide rods assemble into ordered structures, while the flexible chains are spread out into the surroundings to stabilize the structures.

In a recent work, Lin et al. reported the self-assembly behavior of PBLG-*b*-PEG block copolymer in $CHCl_3$/ethanol/TFA mixed solution. In solution, the micelles are formed with PEG as the shell and PBLG as the core [61]. In the absence of TFA, PBLG adopts a rigid α-helix conformation and the block copolymers self-assemble into cylindrical micelles (Fig. 17a). With the introduction of TFA into the solution, the conformation of PBLG transforms from α-helix to random coil and the aggregate morphology transforms to spherical micelles (Fig. 17b). Concomitantly with the changes in morphology, the micelle size tends to become smaller. Further understanding of such a micelle morphology transition induced by polypeptide conformation variation is assisted by a Brownian dynamics (BD) simulation. Based on the experimental and simulation results, a well-founded mechanism regarding the effect of PBLG conformation on the self-assembly behavior was proposed. As shown in Fig. 17c, polypeptide blocks within the cores are interdigitated and favor ordered parallel packing, with their long axis aligning in an orientation vector.

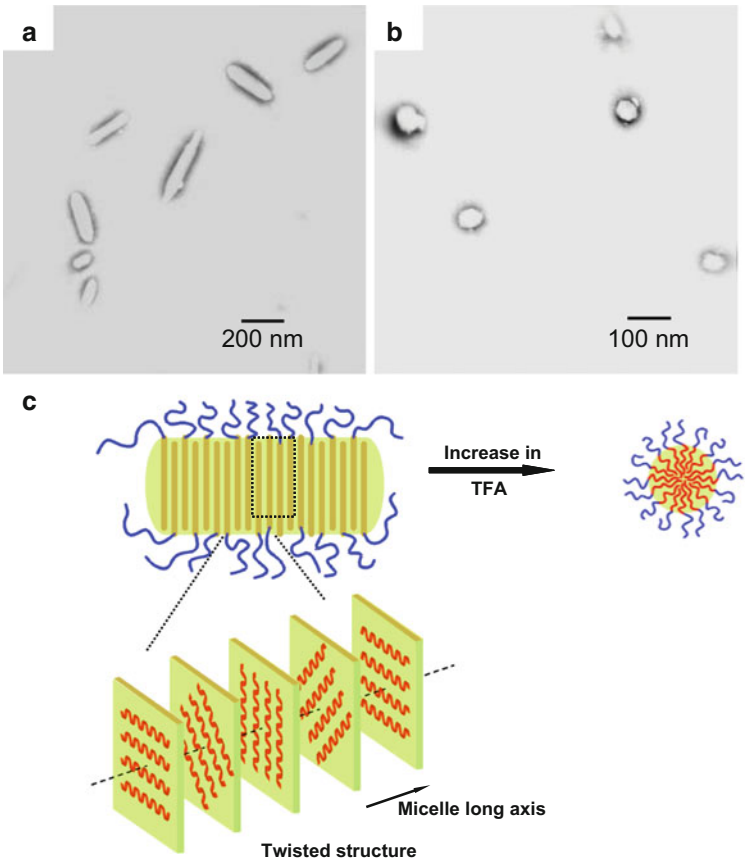

Fig. 17 TEM photographs of PBLG-*b*-PEG micelles formed in (**a**) $CHCl_3$/ethanol solution and (**b**) $CHCl_3$/ethanol/TFA solution. (**c**) Scheme for the aggregate morphology transition from cylinder to sphere as the polypeptide conformation changes from helix to coil. Reprinted with permission from [61]. Copyright 2008 American Chemical Society

The vector could gradually change along the long-center-axis of the micelle in a cholesteric LC manner. Such a packing of the PBLG blocks in the core satisfies the natural tendency toward twisted packing of helical rods and can also maximize the effective volume for the PEG blocks in the micelle shells. The PEG segments relax and laterally form the corona of the micelle to maximize their conformation entropy. When the denaturant acid TFA is added, polypeptide chains become random coils and the regular packing of PBLG blocks in the core is destroyed. As a result, spherical micelles with coiled polypeptide blocks randomly packing inside the cores are formed.

The above example shows that a conformation transition from α-helix to random coil can destroy the ordered packing of polypeptide chains in micelle core, which simultaneously induces a cylinder-to-sphere morphology transition. A similar

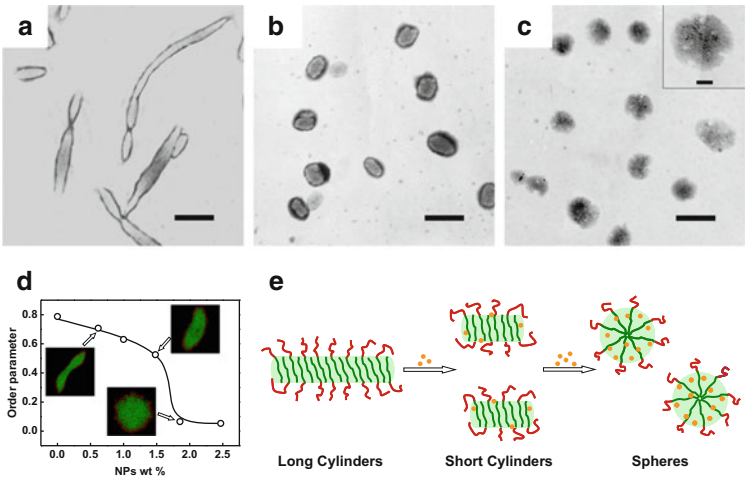

Fig. 18 TEM images of PBLG-*b*-PEG/AuNP hybrid micelles with various AuNP content: (**a**) 0, (**b**) 1, and (**c**) 3 wt%. The *inset* in (**c**) shows a magnified image of hybrid micelles. (**d**) Simulation prediction for the order parameter of rod blocks as a function of the concentration of nanoparticles. The *insets* show the corresponding structures of hybrid micelles. The nanoparticles are not shown for clarity. (**e**) Proposed self-assembly behaviors of PBLG-*b*-PEG/AuNP mixtures. Reprinted with permission from [128]. Copyright 2012 American Chemical Society

micelle morphology transition from cylinder to sphere for the same PBLG-*b*-PEG block copolymers is achieved by adding a small portion of gold nanoparticles (AuNPs), as reported in a recent work by Cai et al. [128]. The main reason for the aggregate morphology transition is the breakage of ordered packing of PBLG rods in the cylindrical micelle core by the added nanoparticles. As shown in Fig. 18a, pure block copolymers form cylindrical micelles in solution of $CHCl_3$/ethanol (v/v = 4/6). When the AuNPs is introduced, as shown in Fig. 18b, short cylinders are produced. These short cylinders have the same diameter as the long cylinders, which indicates that the short cylinders could be fragments of the long cylinders. Further increasing the AuNP content to 2–10 wt% leads to the formation of spherical micelles (Fig. 18c, AuNPs 3 wt%). From the TEM image shown in the inset of Fig. 18c, it can be observed that AuNPs exist in the micelle core. The authors also performed a dissipative particle dynamics (DPD) simulation study on this system. As shown in Fig. 18d, the simulation results from a model system of rod–coil copolymer/nanoparticles reproduced the experimental findings well. In addition, the simulations reveal that with the incorporation of NPs into the micelle core, the ordered packing of rod block in the micelle core is gradually destroyed. The order parameter of the rod block gradually decreases from about 0.8 for cylinders to nearly zero for spherical micelles. Fig. 18e schematically presents the self-assembly behaviors of PBLG-*b*-PEG/AuNPs mixtures. It can be clearly seen that when the weight fraction of NPs is lower, the ordered arrangement of PBLG rods in the micelle core is partially destroyed and short cylinders are

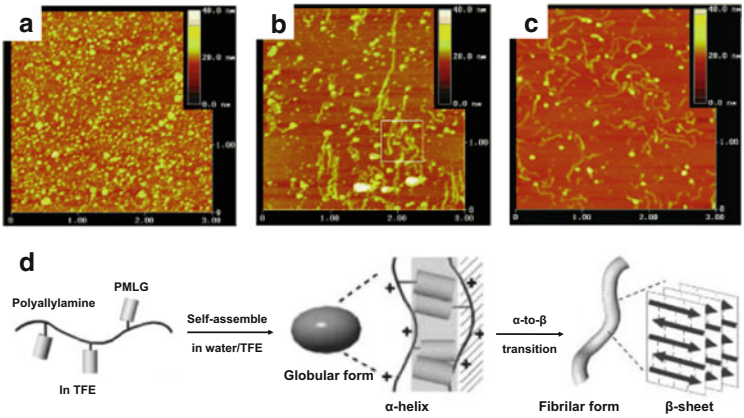

Fig. 19 AFM images showing the time dependent changes in morphology of polyallylamine-*g*-PMLG in water/TFE (8:2 v/v) solution: (**a**) 0 h, (**b**) 5 h, and (**c**) 48 h. (**d**) Morphology and conformation of the graft copolymer. Reprinted with permission from [130]. Copyright 2003 Wiley-VCH

produced. When the weight fraction of NPs increases, the sustaining filling of the nanoparticles destroys the global ordering of the PBLG rods and spherical micelles are formed.

Cylindrical micelles were also observed for graft copolymers with solvophobic polypeptide side chains [129, 130]. For example, Higuchi et al. found that in water/2,2,2-trifluoroethanol (TFE) mixture solution (pH $<$ 8), polyallylamine-*g*-PMLG graft copolymers can first assemble into small globules, and then transform into long fibrils [130]. The aggregate morphology was observed by AFM. As shown in Fig. 19a, when the graft polymer is dispersed in water/TFE mixture solution, globular aggregates are first formed by the strong hydrophobic interaction between PMLG chains. In this stage, PMLG grafts take mainly α-helical form. After incubation for 5 h, fibrils together with globular aggregates are observed (Fig. 19b). After further incubation for 48 h, the major structures were found to be amyloid-like fibrils (Fig. 19c). Such a morphology transition from globules to fibrils is accompanied by a change in the conformation of PMLG from α-helix to β-sheet. The PMLG β-sheets are antiparallel and form fibril structures. Figure 19d schematically illustrates the morphology and PMLG conformation transition of graft copolymer in solutions.

Lin et al. reported that PBLG-*g*-PEG graft copolymers with a rigid polypeptide backbone can self-assemble into spindles and cylindrical micelles in which the PBLG backbones take side-by-side ordered packing with their long axes aligned in a nematic manner, while spread out hydrophilic PEG chains stabilize the aggregates [62, 131]. For a PBLG-*g*-PEG/$CHCl_3$/ethanol solution system, when TFA is introduced the rigid α-helix conformation of the PBLG backbone transforms to a random coil conformation. The flexible polypeptide chains tend to randomly pack in the aggregate core. As a result, spindles transform to large spheres [62].

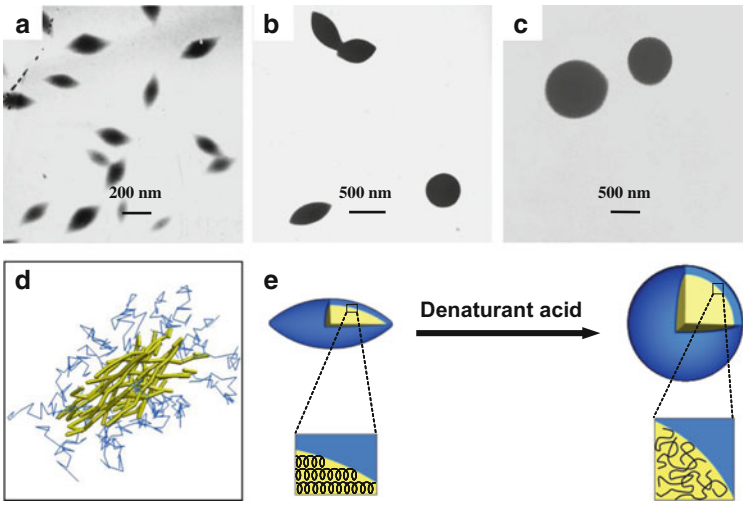

Fig. 20 TEM images of PBLG-*g*-PEG aggregates formed in $CHCl_3$/ethanol/TFA solutions with various TFA mole fractions: (**a**) 0, (**b**) 0.012, and (**c**) 0.016. (**d**) Simulation results of aggregates obtained from rod–coil graft copolymer at rigid conformation fractions of 87.5%. (**e**) Model proposed for the PBLG-*g*-PEG aggregates formed under various conditions. Reprinted with permission from [62]. Copyright 2008 Elsevier

Figure 20a–c shows the TEM images of the PBLG-*g*-PEG graft copolymer aggregates. With no TFA, small spindles are observed (Fig. 20a). At a lower TFA content, the intramolecular H-bonding of PBLG is partially destroyed and thus the PBLG backbone becomes a semi-rigid chain and the PBLG-*g*-PEG graft copolymers self-assemble into a mixture of spindles and spheres (Fig. 20b). With further increase in the TFA content, PBLG becomes random coil and larger spheres are formed by the graft copolymers (Fig. 20c).

Lin and coworkers also carried out a DPD simulation on model graft copolymers with various rigid fractions of the backbone. Figure 20d shows a typical result for the spindle self-assembled from the graft copolymers with a semi-rigid backbone (rigid conformation fraction of backbone is 87.5%). This result captures the essential feature of the structure observed in experiments (Fig. 20b). Some information that is difficult to be gained through experiments can be obtained. For example, an orientational order parameter of the polypeptide backbones of about 0.7 is obtained. Figure 20e illustrates a model proposed for the morphology transition of PBLG-*g*-PEG aggregation as a function of polypeptide backbone conformation.

Combining the experimental and simulation work is an effective strategy for studying complex polymer self-assembly and understanding the mechanism behind the phenomena. On one hand, simulations can not only reproduce the experimental observations, but also provide additional information that is difficult to be obtained from experiments, such as chain orderings and distributions. On the other hand, the validity of the simulation should be tested by comparing the simulation results with experimental observations. If the simulation can only give similar results to those observed experimentally, it tells us no more than that the building model is rational.

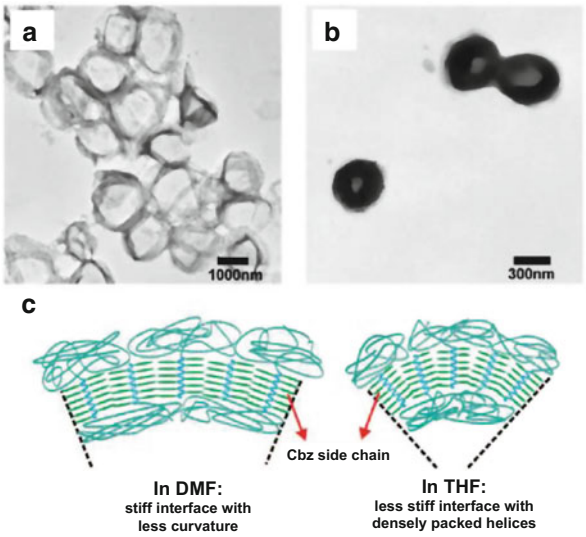

Fig. 21 TEM images of PNIPAm$_{90}$-*b*-PZLys$_{71}$: (**a**) giant vesicles prepared with DMF as initial solvent and (**b**) compact vesicles prepared with THF as initial solvent. (**c**) Proposed self-assembly behaviors. Reprinted with permission from [37]. Copyright 2008 American Chemical Society

In addition to capturing the feature of experimental results, the computer simulations should serve as a tool to give information beyond the experimental observations.

In the above experiments, the simulation results supply missing information like the packing of rigid PBLG and therefore are of significance. However, some aspects of the models were coarse-grained, such as the polydispersity of the polymers and the chiral characteristic of the PBLG. These facts may play an important role in determining the self-assembly behaviors of the present systems, for example, if the chirality of PBLG is incorporated into the model, morphologies with chiral nature would be simulated. This would be an interesting topic for further simulation of the polypeptide systems.

4.2 Vesicles Self-Assembled from Polypeptide Copolymers

Amphiphilic copolymers can self-assemble into vesicles. Polypeptide vesicles have attracted considerable attention due to their large loading capacity and similarity to living cells [10, 132, 133]. The ordered packing of polypeptide chains has also been observed in polypeptide vesicles in which hydrophobic polypeptide chains form the vesicle wall [37, 134–136]. For example, Chang et al. studied the self-assembly behavior of PNIPAm-*b*-PZLys rod–coil block copolymers [37]. They found that by varying the polymer composition and the helicogenic common solvents, these amphiphilic block copolymers were able to form universal aggregate morphologies of spherical micelles, wormlike micelles, and vesicles. For example, PNIPAm$_{91}$-*b*-PZLys$_{71}$ self-assembles into vesicles in water with THF or DMF as initial solvent (Fig. 21a, b). Furthermore, the size of vesicles from DMF/water system is much

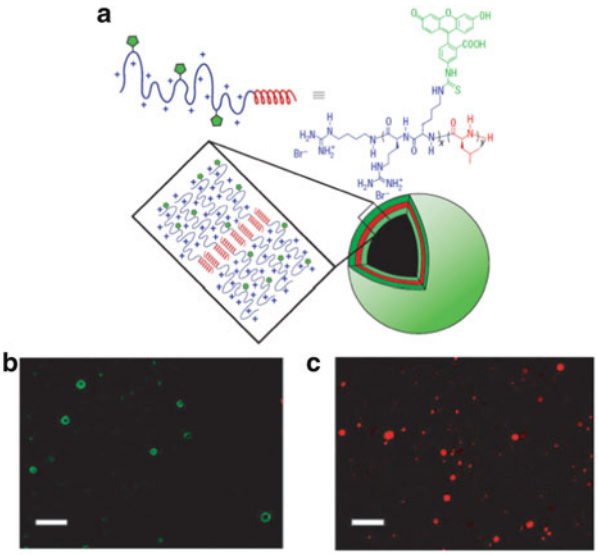

Fig. 22 (**a**) Proposed self-assembly of $PArg_{60}$-*b*-$PLeu_{20}$ vesicles. (**b**) LSCM image of the vesicles. (**c**) LSCM image of the vesicles containing Texas-Red-labeled dextran. Scale bar = 5 μm. Reprinted by permission from Macmillan Publishers Ltd: Nature Materials, [137], copyright (2007)

larger than that from THF/water system. As illustrated in Fig. 21c, polypeptide chains in the vesicle wall take the side-by-side packing mode. Because the dipole moment of DMF is larger than that of THF, when DMF is the initial solvent, the side chain of PZLys possesses a greater dimension, which induces a looser packing of PZLys chains. As a result, the size of the vesicles prepared with DMF as initial solvent is much larger than those prepared with THF.

Deming's group reported a series of work on the polypeptide vesicles formed by copolypeptide amphiphiles of PLL_{60}-*b*-$PLeu_{20}$, $PLGA_{60}$-*b*-$PLeu_{20}$, and $PArg_{60}$-*b*-$PLeu_{20}$ in aqueous solution [46, 137]. For these block copolymers, PLeu is hydrophobic, whereas PLL, PLGA, and PArg are hydrophilic. Vesicle formation is due to a combination of the α-helical hydrophobic segments that favor formation of flat membranes and the highly charged hydrophilic segments that impart solubility and fluidity to these membranes. Typical results from $PArg_{60}$-*b*-$PLeu_{20}$ block copolymers are presented in Fig. 22. Figure 22a shows the proposed vesicle structure from $PArg_{60}$-*b*-$PLeu_{20}$ block polymers. As shown in Fig. 22b, micrometer-sized vesicles in aqueous solution are observed from LSCM. These vesicles are able to entrap water-soluble species, such as dextran. As shown in Fig. 22c, the loading of Texas-Red-labeled dextran in vesicles can be observed.

Up to now, few studies have focused on the formation of vesicles from polypeptide-based graft copolymers. In a recent work, Cai et al. studied the self-assembly behavior of PBLG-*g*-PEG graft copolymers [138]. The degree of grafting of short PEG (M_n = 750) is low (0.28 mol%). With THF as the initial solvent, the graft copolymers self-assemble into vesicles, as shown in Fig. 23a. The three-dimesional SEM image in the inset of Fig. 23a confirms the vesicular structure. It is the first report of the formation of polymeric vesicles from graft copolymers with a rigid polypeptide backbone. When DMF, a better solvent for PBLG than THF, is

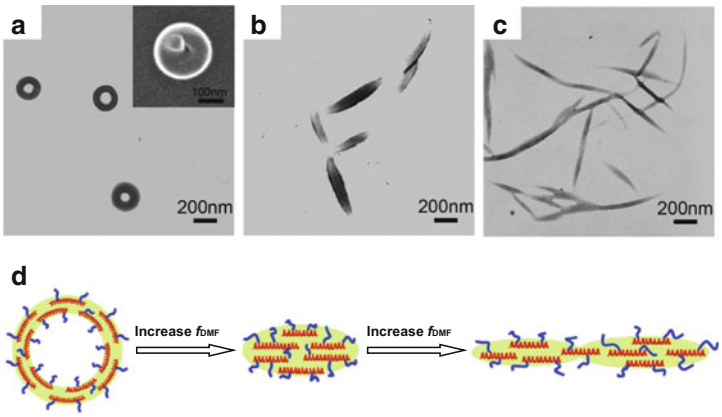

Fig. 23 TEM images of PBLG-*g*-PEG graft copolymer aggregates as a function of initial common solvents: (**a**) THF; (**b**) THF/DMF at 1/1 v/v; (**c**) DMF. (**d**) Aggregation as a function of the initial solvent composition. The *inset* in (**a**) is a magnified SEM image of the vesicle. Reprinted with permission from [138]. Copyright 2010 American Chemical Society

introduced into the initial solvent, the aggregate morphology transforms to spindles and connected spindles (see Fig. 23b–c). For the vesicles, PBLG backbones should align in ordered packing and bend in the wall of the vesicle. Because of the imperfect nature of the PBLG helices, such a bended state of the PBLG chains can be achieved without raising the system energy markedly. In addition, such a packing mode prevents the exposing of the PBLG chain to water. While in the spindles and connected spindles, PBLG chains are believed to take a dislocated side-by-side packing manner. Figure 23d is a schematic illustration of the aggregation as a function of the initial solvent composition. Polypeptide graft copolymers have obvious advantages in adjusting the self-assembly behavior by changing the side-chain properties, such as grafting density, chain length, environmental sensitivity, etc. Thus these polypeptide-based vesicles may be potential candidates for drug carriers and the like.

In a subsequent work, Cai et al. investigated the effect of PBLG-*b*-PEG block copolymer on the self-assembly of the PBLG-*g*-PEG graft copolymers [139]. They found that the cooperative self-assembly of mixtures containing vesicle-forming PBLG-*g*-PEG graft copolymers and vesicle- or micelle-forming PBLG-*b*-PEG block copolymers always produces cylindrical micelles (Fig. 24). For the hybrid cylinders, block copolymers are found to mainly locate at the ends of the aggregates, which prevents the fusion of cylinders to vesicles in the assembly process. Thus, the cylindrical structure is preserved by removing organic solvent. These results are not only beneficial to understanding the formation of vesicles from polypeptide-based graft copolymers, but also enrich our knowledge of the self-assembly of multicomponent systems.

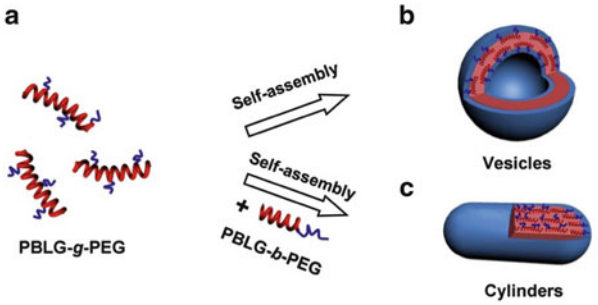

Fig. 24 Self-assembly of polypeptide-based block and graft copolymer mixtures. Reprinted with permission from [139]. Copyright 2012 American Chemical Society

4.3 Complex Structures Self-Assembled from Polypeptide Copolymers

In addition to the cylindrical micelles and vesicles, the ordering of polypeptide chains also contributes to the formation of complex structures with hierarchical feature [140–142]. For example, Nolte et al. found that the polypeptide-based block copolymers of polystyrene with poly(isocyano-L-alanine-L-alanine) and poly (isocyano-L-alanine-L-histidine), PS_{40}-*b*-$PIAA_{10}$ (Fig. 25a) and PS_{40}-*b*-$PIAH_{15}$ (Fig. 25b), are able to self-assemble into super-helical structures in a sodium acetate buffer of pH 5.6 (0.2 mM) [140]. Structures with two length-scales are involved in such super-helices: fiber-like whole structures and screws of the super-helices. As shown in Fig. 25c–e, the super-helices have an opposite chirality to that of the constituent polypeptide segments of building block copolymers. Since the polypeptide chains take rigid α-helix conformation and the chirality of the formed super-helices is related to the handedness of the building polypeptides, it can be deduced that the ordering of polypeptide rods is an important factor in determining the formation of these hierarchical structures.

As reported by Cai et al., virus-like right-handed super-helical fibers and rings can be self-assembled from a binary system consisting of rod–coil PBLG-*b*-PEG block copolymers and PBLG rigid homopolymers [141]. The hierarchical structures are formed with PBLG bundles as the core wrapped by PBLG-*b*-PEG block copolymers. They revealed that the high molecular weight of PBLG homopolymer is crucial for the construction of the super-helical structures. For the mixture system containing low molecular weight PBLG homopolymers ($PBLG_{40000}$), spheres are observed (Fig. 26a). With increasing molecular weight of the PBLG homopolymers ($PBLG_{110000}$), super-helical rods start to appear (Fig. 26b). With further increase in the molecular weight of homo-PBLG ($PBLG_{520000}$), long super-helical fibers and rings with uniform diameter of 140 nm and screw-pitch of 80 nm are obtained (Fig. 26c). The detailed surface profile of the super-helices was examined using AFM analysis. As shown in

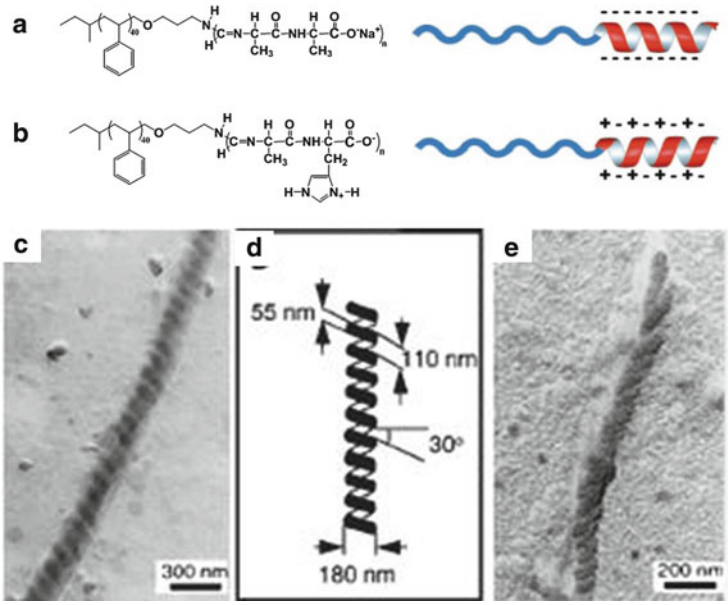

Fig. 25 Polymer structures of (**a**) PS_{40}-*b*-$PIAA_{10}$, right-handed polypeptide backbone and (**b**) PS_{40}-*b*-$PIAH_{15}$, left handed polypeptide backbone. (**c**) Left-handed super-helix from PS_{40}-*b*-$PIAA_{10}$. (**d**) Representation of the helix in (**c**). (**e**) Right-handed super-helical aggregate formed by PS_{40}-*b*-$PIAH_{15}$. From [140]. Reprinted with permission from AAAS

Fig. 26d, the width and screw pitch of the assemblies are similar to those observed in SEM images. The orientation of the height contour indicates that these super-helices have a right-handed sense. Many possible interactions, including hydrophobic, dipolar π–π interactions, and ordered packing tendency of α-helical polypeptide segments, are believed to be responsible for the formation of super-helical structures.

Usually, hierarchical structure-forming systems contain complex interactions, thus it is a daunting task to understand exactly how the observed structures were formed. Computer simulation is a useful tool for investigating multicomponent self-assembly systems and elucidating the supramolecular structures. Cai et al. also carried out a BD simulation on a model rod–coil block copolymer/rigid homopolymer binary system. From the simulation results, it was found that the homopolymers and block copolymers formed ordered structures with different scales. The polypeptide homopolymers packed side-by-side to form bundles; the block copolymers were helically wrapped on the homopolymer bundles; and the packing mode of block PBLG rods exhibited characteristics of the cholesteric LC structure. In such a structure, there exist two levels of polypeptide chain ordering. The interplay of these two level orderings has an important role in determining the final structures.

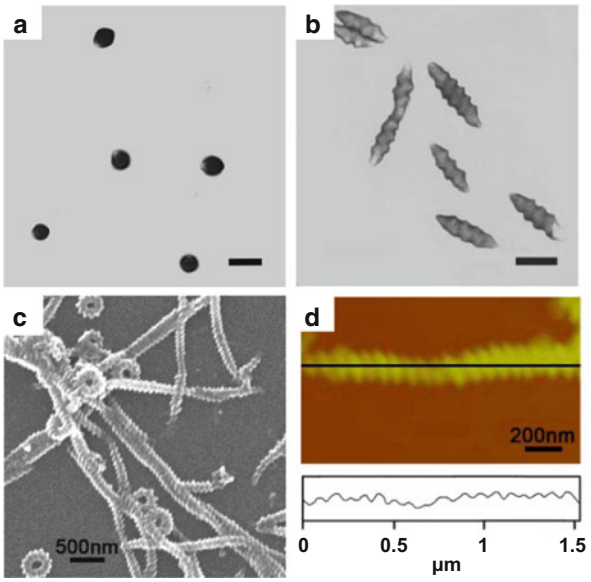

Fig. 26 (**a**) TEM image of spheres self-assembled from PBLG-*b*-PEG/$PBLG_{40000}$. (**b**) TEM image of super-helical rods self-assembled from PBLG-*b*-PEG/$PBLG_{110000}$. (**c**) SEM image of super-helical fibers and rings self-assembled from PBLG-*b*-PEG/$PBLG_{520000}$. (**d**) AFM images length profile of super-helical fibers self-assembled from PBLG-*b*-PEG/$PBLG_{520000}$. Reproduced from [141] with permission of The Royal Society of Chemistry

In this work, Cai et al. presented a simple strategy for preparation of polypeptide hierarchical super-helical structures by self-assembly of block copolymer and homopolymer mixtures. The helices have a PBLG bundle covered by PBLG-*b*-PEG chains, which is reminiscent of the structure of tobacco mosaic virus (RNA in the core, covered with a protein shell). This progress is promising for the construction of complicated biological analogs such as a model virus and subsequent investigation of its physiological behavior, e.g., cell penetration of the virus. Therefore, understanding the self-assembly of the mixture system is important and may become a focus of future research [121].

5 Concluding Remarks and Outlook

Polypeptides can take rigid form with an intramolecularly H-bonded α-helix conformation, which enables polypeptide homopolymers and copolymers to assemble into ordered structures by the orderly packing of polypeptide segments in both concentrated and dilute solutions. In addition, the intermolecularly H-bonded β-sheet conformation facilitates the formation of ordered structures, especially gels in solution. Ordered packing of polypeptide segments makes polypeptide

homopolymers and copolymers assemble into distinct structures. Great efforts have been made to construct polypeptide-based assemblies with ordered domains formed by polypeptide chains.

LCs were the earliest studied structures, in which polypeptide homopolymer rods pack in an ordered manner to form smectic, nematic, and cholesteric phases. The smectic LCs are mainly formed by polypeptide homopolymers with identical polymer length. The cholesteric phase can be prepared by synthetic polypeptides with polydisperse chain length. The nematic phase can be regarded as a special example of the cholesteric phase with an infinite cholesteric pitch. The cholesteric pitch and chirality in the polypeptide LCs are dependent on many factors, such as temperature, polymer concentration, solvent nature, and polypeptide conformation. Deep understanding of such phenomena is necessary for preparation of ordered polypeptide assembles with delicate structures. The addition of denaturing solvent to polypeptide solution can lead to an anisotropic–isotropic reentrant transition at low temperatures where the intramolecular helix–coil transformation occurs. However, the helical structure is more stable in LC phase than in dilute solution due to the conformational ordering effect.

Gels have attracted considerable attention for a long time. In polypeptide homopolymer gels, polypeptides assemble into fiber structures with dislocated side-by-side packing of rods. Thus, they possess a similar structure to LC structures; however, the order parameter is relatively lower. For polypeptide block copolymers, gels are formed with packing of polypeptide chains, while the other flexible chains are spread out into the surrounding to stabilize the gels in solution. Both the α-helix and β-sheet conformation of polypeptides support the formation of gels through inter- and intramolecular attractions. The gels formed from β-sheet polypeptides are found to have higher strength than those formed by α-helix polypeptides. However, most of the gels, especially the hydrogels, are still not strong enough for practical applications. Modified hydrophilic polypeptides are promising for the preparation of strong hydrogels. It is fundamentally important to construct gels with controlled structures and morphologies for diverse applications in the fields of template synthesis, functional materials, and tissue engineering scaffolds.

The ordered packing of polypeptides can be also found in copolymer micelles self-assembled in dilute solutions. The ordering tendency of polypeptide segments is favorable for the formation of cylindrical micelles, large vesicles, and hierarchical structures. The formed structures show higher stabilities due to the ordering within domains in the assemblies. Introducing a second component, including polymers and nanoparticles, is an effective way to adjust the self-assembly behavior of parent block and graft copolymers. The conformation transition of the polypeptide chains is also an important factor affecting the assembly behavior of polypeptide copolymers. The study of hierarchical structures of polypeptides is an especially attractive and promising topic because polypeptides are the fundamental building blocks for fabricating hierarchical structures in living organisms. Such hierarchical structures usually show chirality. Further work eliciting the relationship between handedness of the polypeptides and the chirality of the formed hierarchical

structures is highly desired. In addition, development in such fields will open a door to the preparation of advanced functional biomaterials, which is eagerly demanded in medicaland biorelated areas.

It is evident that the bioapplication of polypeptide assemblies is one of the most promising and important directions for research. Based on the ordering packing of polypeptide segments with α-helix and β-sheet conformations, novel superstructures in the forms of LCs, gels, and micelles have been sucessfully created. Although started about 60 years ago in the late 1940s, the ordering of polypeptides in the fabrication of diverse structures is still at a early stage. The assembly mechanisms behind the phenomena for LCs, gels, and micelles have not been well understood. The combination of experiments with computer simulations is a promising strategy for unveiling the fundamental principles of polypeptide assembly behavior. The application potential of the polypeptide assemblies has also not been well evaluated. More research is needed to implement the applications of polypeptide assemblies, which will further push the advance of polypeptide assembly research. Moreover, since polypeptides resemble proteins in structure, mimicking proteins is a charming aspect of polypeptide research, which could be helpful for investigating complex protein systems.

Acknowledgements This work was supported by National Natural Science Foundation of China (50925308 and 21234002), Key Grant Project of Ministry of Education (313020), and National Basic Research Program of China (No. 2012CB933600). Support from projects of Shanghai municipality (10GG15 and 12ZR1442500) is also appreciated.

References

1. Deming TJ (1997) Polypeptide materials: new synthetic methods and applications. Adv Mater 9:299–311
2. Mart RJ, Osborne RD, Stevens URV (2006) Peptide-based stimuli-responsive biomaterials. Soft Matter 2:822–835
3. Osada K, Kataoka K (2006) Drug and gene delivery based on supramolecular assembly of PEG-polypeptide hybrid block copolymers. Adv Polym Sci 202:113–153
4. Schlaad H (2006) Solution properties of polypeptide-based copolymers. Adv Polym Sci 202:53–73
5. Carlsen A, Lecommandoux S (2009) Self-assembly of polypeptide-based block copolymer amphiphiles. Curr Opin Colloid Interface Sci 14:329–339
6. Deming TJ (2007) Synthetic polypeptides for biomedical applications. Prog Polym Sci 32:858–875
7. Banwell EF, Abelardo ES, Adams DJ, Birchall MA, Corrigan A (2009) Rational design and application of responsive α-helical peptide hydrogels. Nat Mater 8:596–600
8. He C, Zhuang X, Tang Z, Tian H, Chen X (2012) Stimuli-sensitive synthetic polypeptide-based materials for drug and gene delivery. Adv Healthc Mater 1:48–78
9. Lowik DWPM, Leunissen EHP, van den Heuvel M, Hansen MB, van Hest JCM (2010) Stimulus responsive peptide based materials. Chem Soc Rev 39:3394–3412
10. Choe U-J, Sun VZ, Tan JKY, Kamei DT (2012) Self-assembly polypeptide and polypeptide hybrid vesicles: from synthesis to application. Top Curr Chem 310:117–134

11. Chow D, Nunalee ML, Lim DW, Simnick AJ, Chilkoti A (2008) Peptide-based biopolymers in biomedicine and biotechnology. Mater Sci Eng R Rep 62:125–155
12. Lim Y-b, Lee E, Lee M (2007) Cell-penetrating-peptide-coated nanoribbons for intracellular nanocarriers. Angew Chem Int Ed 46:3475–3478
13. Kopecek J, Yang J (2012) Smart self-assembled hybrid hydrogel biomaterials. Angew Chem Int Ed 51:7396–7417
14. Higashihara T, Ueda M (2011) Block copolymers containing rod segments. In: Hadjichristidis N, Hirao A, Tezuka Y, Du Prez F (eds) Complex macromolecular architectures: synthesis, characterization, and self-assembly. Wiley, Hoboken, pp 395–429
15. Klok H-A (2002) Protein-inspired materials: synthetic concepts and potential applications. Angew Chem Int Ed 41:1509–1513
16. Zhang G, Fournier MJ, Mason TL, Tirrell DA (1992) Biological synthesis of monodisperse derivatives of poly(α, L-glutamic acid): model rodlike polymers. Macromolecules 25:3601–3603
17. Rabotyagova OS, Cebe P, Kaplan DL (2011) Protein-based block copolymers. Biomacromolecules 12:269–289
18. Kiick KL (2002) Genetic methods of polymer synthesis. In: Mark HF (ed) Encyclopedia of polymer science and technology. Wiley, Hoboken, pp 515–522
19. Merrifield RB (1963) Solid phase peptide synthesis. I. The synthesis of a tetrapeptide. J Am Chem Soc 85:2149–2154
20. Aliferis T, Iatrou H, Hadjichristidis N (2004) Living polypeptides. Biomacromolecules 5:1653–1656
21. Hadjichristidis N, Iatrou H, Pitsikalis M, Sakellariou G (2009) Synthesis of well-defined polypeptide-based materials via the ring-opening polymerization of alpha-amino acid *N*-carboxyanhydrides. Chem Rev 109:5528–5578
22. Kricheldorf HR (2006) Polypeptides and 100 years of chemistry of α-amino acid *N*-carboxyanhydrides. Angew Chem Int Ed 45:5752–5784
23. Kricheldorf HR (1987) α-aminoacid-*N*-carboxy-anhydrides and related heterocycles: syntheses, properties, peptide synthesis, polymerization. Springer, Berlin
24. Penczek S, Kricheldorf HR (1990) Models of biopolymers by ring opening polymerization. CRC, Boca Raton
25. Duran H, Ogura K, Nakao K, Vianna SDB, Usui H (2009) High-vacuum vapor deposition and in situ monitoring of *N*-carboxy anhydride benzyl glutamate polymerization. Langmuir 25:10711–10718
26. Leuchs H, Geiger W (1908) The anhydrides of alpha-amino-*N*-carboxylic and alpha-amino acids. Ber Dtsch Chem Ges 41:1721–1726
27. Voet D, Voet JG (eds) (1995) Biochemistry, Solutions Manual. Wiley, Hoboken
28. Zimm BH, Bragg JK (1959) Theory of the phase transition between helix and random coil in polypeptide chains. J Chem Phys 31:526–535
29. Teramoto A, Fujita H (1975) Conformation-dependent properties of synthetic polypeptides in the helix-coil transition region. Adv Polym Sci 18:65–149
30. Parras P, Castelletto V, Hamley IW, Klok H-A (2005) Nanostructure formation in poly (γ-benzyl-L-glutamate)-poly(ethylene glycol)-poly(γ-benzyl-L-glutamate) triblock copolymers in the solid state. Soft Matter 1:284–291
31. Hadjichristidis N, Iatrou H, Pitsikalis M, Pispas S, Avgeropoulos A (2005) Linear and non-linear triblock terpolymers: synthesis, self-assembly in selective solvents and in bulk. Prog Polym Sci 30:725–782
32. Klok H-A, Lecommandoux S (2006) Solid-state structure, organization and properties of peptide-synthetic hybrid block copolymers. Adv Polym Sci 202:75–111
33. Sanchez-Ferrer A, Mezzenga R (2010) Secondary structure-induced micro- and macrophase separation in rod-coil polypeptide diblock, triblock, and star-block copolymers. Macromolecules 43:1093–1100

34. Babin J, Taton D, Brinkmann M, Lecommandoux S (2008) Synthesis and self-assembly in bulk of linear and mikto-arm star block copolymers based on polystyrene and poly(glutamic acid). Macromolecules 41:1384–1392
35. Kopecek J, Yang J (2009) Peptide-directed self-assembly of hydrogels. Acta Biomater 5:805–816
36. Hermes F, Otte K, Brandt J, Grawert M, Borner HG, Schlaad H (2011) Polypeptide-based organogelators: effects of secondary structure. Macromolecules 44:7489–7492
37. Huang C-J, Chang F-C (2008) Polypeptide diblock copolymers: syntheses and properties of poly(*N*-isopropylacrylamide)-b-polylysine. Macromolecules 41:7041–7052
38. Gebhardt KE, Ahn S, Venkatachalam G, Savin DA (2008) Role of secondary structure changes on the morphology of polypeptide-based block copolymer vesicles. J Colloid Interface Sci 317:70–76
39. Robinson C (1956) Liquid-crystalline structures in solutions of a polypeptide. Trans Faraday Soc 52:571–592
40. Uematsu I, Uematsu Y (1984) Polypeptide liquid crystals. Adv Polym Sci 59:37–73
41. Flory PJ, Leonard WJ (1965) Thermodynamic properties of solutions of helical polypeptides. J Am Chem Soc 87:2102–2108
42. Tohyama K, Miller WG (1981) Network structure in gels of rod-like polypeptides. Nature 289:813–814
43. Cohen Y (1996) The microfibrillar network in gels of poly(γ-benzyl-L-glutamate) in benzyl alcohol. J Polym Sci, Part B: Polym Phys 34:57–64
44. Kim KT, Park C, Vandermeulen GWM, Rider DA, Kim C, Winnik MA, Manners I (2005) Gelation of helical polypeptide-random coil diblock copolymers by a nanoribbon mechanism. Angew Chem Int Ed 44:7964–7968
45. Rodriguez-Hernandez J, Lecommandoux S (2005) Reversible inside-out micellization of pH-responsive and water-soluble vesicles based on polypeptide diblock copolymers. J Am Chem Soc 127:2026–2027
46. Holowka EP, Pochan DJ, Deming TJ (2005) Charged polypeptide vesicles with controllable diameter. J Am Chem Soc 127:12423–12428
47. Bellomo EG, Wyrsta MD, Pakstis L, Pochan DJ, Deming TJ (2004) Stimuli-responsive polypeptide vesicles by conformation-specific assembly. Nat Mater 3:244–248
48. Kim KT, Park C, Kim C, Winnik MA, Manners I (2006) Self-assembly of dendron-helical polypeptide copolymers: organogels and lyotropic liquid crystals. Chem Commun 1372–1374
49. Yu SM, Conticello VP, Zhang G, Kayser C, Fournier MJ, Mason TL, Tirrell DA (1997) Smectic ordering in solutions and films of a rod-like polymer owing to monodispersity of chain length. Nature 389:167–170
50. Schmidtke S, Russo P, Nakamatsu J, Buyuktanir E, Turfan B, Temyanko E, Negulescu I (2000) Thermoreversible gelation of isotropic and liquid crystalline solutions of a "sticky" rodlike polymer. Macromolecules 33:4427–4432
51. Ginzburg B, Siromyatnikova T, Frenkel S (1985) Gelation in the poly(γ-benzyl-L-glutamate)-dimethylformamide system. Polym Bull (Berl) 13:139–144
52. Russo PS, Magestro P, Miller WG (1987) Gelation of poly(γ-benzyl-α,L-glutamate). In: Russo PS (ed) Reversible polymeric gels and related systems. ACS symposium series, vol 350. American Chemical Society, Washington, DC, pp 152–180
53. Kuo S-W, Lee H-F, Huang W-J, Jeong K-U, Chang F-C (2009) Solid state and solution self-assembly of helical polypeptides tethered to polyhedral oligomeric silsesquioxanes. Macromolecules 42:1619–1626
54. Kim EH, Joo MK, Bahk KH, Park MH, Chi B, Lee YM, Jeong B (2009) Reverse thermal gelation of PAF-PLX-PAF block copolymer aqueous solution. Biomacromolecules 10:2476–2481
55. Li T, Lin J, Chen T, Zhang S (2006) Polymeric micelles formed by polypeptide graft copolymer and its mixtures with polypeptide block copolymer. Polymer 47:4485–4489

56. Cai C, Zhang L, Lin J, Wang L (2008) Self-assembly behavior of pH- and thermosensitive amphiphilic triblock copolymers in solution: experimental studies and self-consistent field theory simulations. J Phys Chem B 112:12666–12673
57. Ueda M, Makino A, Imai T, Sugiyama J, Kimura S (2011) Transformation of peptide nanotubes into a vesicle via fusion driven by stereo-complex formation. Chem Commun 47:3204–3206
58. Cai C, Wang L, Lin J (2011) Self-assembly of polypeptide-based copolymers into diverse aggregates. Chem Commun 47:11189–11203
59. Kim MS, Dayananda K, Choi EY, Park HJ, Kim JS, Lee DS (2009) Synthesis and characterization of poly(L-glutamic acid)-block-poly(L-phenylalanine). Polymer 50:2252–2257
60. Schenck HL, Gellman SH (1998) Use of a designed triple-stranded antiparallel β-sheet to probe β-sheet cooperativity in aqueous solution. J Am Chem Soc 120:4869–4870
61. Ding W, Lin S, Lin J, Zhang L (2008) Effect of chain conformational change on micelle structures: experimental studies and molecular dynamics simulations. J Phys Chem B 112:776–783
62. Lin J, Zhu G, Zhu X, Lin S, Nose T, Ding W (2008) Aggregate structure change induced by intramolecular helix-coil transition. Polymer 49:1132–1136
63. Kotharangannagari VK, Sanchez-Ferrer A, Ruokolainen J, Mezzenga R (2012) Thermoreversible gel–sol behavior of rod-coil-rod peptide-based triblock copolymers. Macromolecules 45:1982–1990
64. Yu SM, Soto CM, Tirrell DA (2000) Nanometer-scale smectic ordering of genetically engineered rodlike polymers: synthesis and characterization of monodisperse derivatives of poly(γ-benzyl α, L-glutamate). J Am Chem Soc 122:6552–6559
65. Sasaki S, Tokuma K, Uematsu I (1983) Phase behavior of poly(γ-benzyl L-glutamate) solutions in benzyl alcohol. Polym Bull (Berl) 10:539–546
66. Watanabe J, Takashina Y (1991) Columnar liquid crystals in polypeptides. 1. A columnar hexagonal liquid crystal observed in poly(γ-octadecyl L-glutamate). Macromolecules 24:3423–3426
67. Robinson C, Ward JC (1957) Liquid-crystalline structures in polypeptides. Nature 180:1183–1184
68. Robinson C (1961) Liquid-crystalline structures in polypeptide solutions. Tetrahedron 13:219–234
69. Robinson C, Ward JC, Beevers RB (1958) Liquid crystalline structure in polypeptide solutions. Part 2. Discuss Faraday Soc 25:29–42
70. Samulski ET, Tobolsky AV (1967) Solid "liquid crystal" films of poly-γ-benzyl-L-glutamate. Nature 216:997
71. Elliott A, Ambrose EJ (1950) Evidence of chain folding in polypeptides and proteins. Discuss Faraday Soc 9:246–251
72. Marx A, Thiele C (2009) Orientational properties of poly-γ-benzyl-L-glutamate: influence of molecular weight and solvent on order parameters of the solute. Chem Eur J 15:254–260
73. Watanabe J, Nagase T (1988) Thermotropic polypeptides. 5. Temperature dependence of cholesteric pitches exhibiting a cholesteric sense inversion. Macromolecules 21:171–175
74. Toriumi H, Kusumi Y, Uematsu I, Uematsu Y (1979) Thermally induced inversion of the cholesteric sense in lyotropic polypeptide liquid crystals. Polym J 11:863–869
75. Toriumi H, Minakuchi S, Uematsu Y, Uematsu I (1980) Helical twisting power of poly (γ-benzyl-L-glutamate) liquid crystals in mixed solvents. Polym J 12:431–437
76. Abe A, Hiraga K, Imada Y, Hiejima T, Furuya H (2005) Screw-sense inversion characteristic of α-helical poly(β-p-chlorobenzyl L-aspartate) and comparison with other related polyaspartates. Peptide Sci 80:249–257
77. Abe A, Furuya H, Okamoto S (1997) Spatial configurations, transformation, and reorganization of mesophase structures of polyaspartates-a highly intelligent molecular system. Peptide Sci 43:405–412

78. Abe A, Imada Y, Furuya H (2010) Mechanism of the screw-sense reversal of tightly hydrogen-bonded α-helical network triggered by the side-chain conformation. Polymer 51:6234–6239
79. Junnila S, Houbenov N, Hanski S, Iatrou H, Hirao A, Hadjichristidis N, Ikkala O (2010) Hierarchical smectic self-assembly of an ABC miktoarm star terpolymer with a helical polypeptide arm. Macromolecules 43:9071–9076
80. Lin J (1997) Re-entrant isotropic transition of polypeptide liquid crystal. Polymer 38:4837–4841
81. Lin J (1998) Reentrant isotropic transition of polypeptide liquid crystal: effect of steric and orientation–dependent interactions. Polymer 39:5495–5500
82. Lin J, Abe A, Furuya H, Okamoto S (1996) Liquid crystal formation coupled with the coil-helix transition in the ternary system poly(γ-benzyl L-glutamate)/dichloroacetic acid/dichloroethane. Macromolecules 29:2584–2589
83. Lin J, Lin S, Liu P, Hiejima T, Furuya H, Abe A (2003) Phase behavior of ternary systems involving a conformationally variable chain and a randomly coiled polymer. Macromolecules 36:6267–6272
84. Flory PJ (1984) Molecular theory of liquid crystals. Adv Polym Sci 59:1–36
85. Abe A, Ballauff M (1991) The Flory lattice model. In: Ciferri A (ed) Liquid crystallinity in polymers: principles and fundamental properties. Wiley-VCH, Weinheim, Chap. 4
86. Lin J, Lin S, Zhang L, Nose T (2009) Microphase separation of rod-coil diblock copolymer in solution. J Chem Phys 130:094907
87. Watanabe J, Imai K, Uematsu I (1978) Light scattering studies of poly(γ-benzyl L-glutamate) solutions and films. Polym Bull 1:67–72
88. Tadmor R, Khalfin RL, Cohen Y (2002) Reversible gelation in isotropic solutions of the helical polypeptide poly(γ-benzyl-L-glutamate): kinetics and formation mechanism of the fibrillar network. Langmuir 18:7146–7150
89. Tipton DL, Russo PS (1996) Thermoreversible gelation of a rodlike polymer. Macromolecules 29:7402–7411
90. Oikawa H, Nakanishi H (2001) Dynamics of probe particles during sol–gel transition of PBLG-DMF solution and the resulting gel structure. J Chem Phys 115:3785–3791
91. Niehoff A, Mantion A, McAloney R, Huber A (2013) Elucidation of the structure of poly (γ-benzyl-L-glutamate) nanofibers and gel networks in a helicogenic solvent. Colloid Polym Sci 291:1353–1363
92. Kishi R, Sisido M, Tazuke S (1990) Liquid-crystalline polymer gels. 1. Cross-linking of poly (γ-benzyl L-glutamate) in the cholesteric liquid-crystalline state. Macromolecules 23:3779–3784
93. Kishi R, Sisido M, Tazuke S (1990) Liquid-crystalline polymer gels. 2. Anisotropic swelling of poly(γ-benzyl L-glutamate) gel crosslinked under a magnetic field. Macromolecules 23:3868–3870
94. Inomata K, Iguchi Y, Mizutani K, Sugimoto H, Nakanishi E (2012) Anisotropic swelling behavior induced by helix-coil transition in liquid crystalline polypeptide gels. ACS Macro Lett 1:807–810
95. Gibson MI, Cameron NR (2008) Organogelation of sheet-helix diblock copolypeptides. Angew Chem Int Ed 47:5160–5162
96. Choi YY, Jeong Y, Joo MK, Jeong B (2009) Reverse thermal organogelation of poly(ethylene glycol)-polypeptide diblock copolymers in chloroform. Macromol Biosci 9:869–874
97. Naik SS, Savin DA (2009) Poly(Z-lysine)-based organogels: effect of interfacial frustration on gel strength. Macromolecules 42:7114–7121
98. Sun J, Chen X, Guo J, Shi Q, Xie Z, Jing X (2009) Synthesis and self-assembly of a novel Y-shaped copolymer with a helical polypeptide arm. Polymer 50:455–461
99. You Y, Chen Y, Hua C, Dong C (2010) Synthesis and thermoreversible gelation of dendron-like polypeptide/linear poly(ε-caprolactone)/dendron-like polypeptide triblock copolymers. J Polym Sci A Polym Chem 48:709–718

100. Borner HG, Smarsly BM, Hentschel J, Rank A, Schubert R, Geng Y, Discher DE, Hellweg T, Brandt A (2008) Organization of self-assembled peptide–polymer nanofibers in solution. Macromolecules 41:1430–1437
101. van Bommel KJC, Friggeri A, Shinkai S (2003) Organic templates for the generation of inorganic materials. Angew Chem Int Ed 42:980–999
102. Sone ED, Zubarev ER, Stupp SI (2002) Semiconductor nanohelices templated by supramolecular ribbons. Angew Chem Int Ed 41:1705–1709
103. Estroff LA, Addadi L, Weiner S, Hamilton AD (2004) An organic hydrogel as a matrix for the growth of calcite crystals. Org Biomol Chem 2:137–141
104. Shumburo A, Biewer MC (2002) Stabilization of an organic photochromic material by incorporation in an organogel. Chem Mater 14:3745–3750
105. Deming TJ (2005) Polypeptide hydrogels via a unique assembly mechanism. Soft Matter 1:28–35
106. Breedveld V, Nowak AP, Sato J, Deming TJ, Pine DJ (2004) Rheology of block copolypeptide solutions: hydrogels with tunable properties. Macromolecules 37:3943–3953
107. Nowak AP, Breedveld V, Pakstis L, Ozbas B, Pine DJ, Pochan D, Deming TJ (2002) Rapidly recovering hydrogel scaffolds from self-assembling diblock copolypeptide amphiphiles. Nature 417:424–428
108. Nowak AP, Breedveld V, Pine DJ, Deming TJ (2003) Unusual salt stability in highly charged diblock co-polypeptide hydrogels. J Am Chem Soc 125:15666–15670
109. Pakstis LM, Ozbas B, Hales KD, Nowak AP, Deming TJ, Pochan D (2003) Effect of chemistry and morphology on the biofunctionality of self-assembling diblock copolypeptide hydrogels. Biomacromolecules 5:312–318
110. Oliveira ED, Hirsch SG, Spontak RJ, Gehrke SH (2003) Influence of polymer conformation on the shear modulus and morphology of polyallylamine and poly(α-L-lysine) hydrogels. Macromolecules 36:6189–6201
111. Choi BG, Park MH, Cho S-H, Joo MK, Oh HJ, Kim EH, Park K, Han DK, Jeong B (2011) Thermal gelling polyalanine–poloxamine–polyalanine aqueous solution for chondrocytes 3D culture: initial concentration effect. Soft Matter 7:456–462
112. Chen Y, Pang X, Dong C (2010) Dual stimuli-responsive supramolecular polypeptide-based hydrogel and reverse micellar hydrogel mediated by host-guest chemistry. Adv Funct Mater 20:579–586
113. Cheng Y, He C, Xiao C, Ding J, Zhuang X, Huang Y, Chen X (2012) Decisive role of hydrophobic side groups of polypeptides in thermosensitive gelation. Biomacromolecules 13:2053–2059
114. Altunbas A, Pochan D (2012) Peptide-based and polypeptide-based hydrogels for drug delivery and tissue engineering. Adv Polym Sci 310:135–167
115. Aggeli A, Nyrkova IA, Bell M, Harding R, Carrick L, McLeish TCB, Semenov AN, Boden N (2001) Hierarchical self-assembly of chiral rod-like molecules as a model for peptide β-sheet tapes, ribbons, fibrils, and fibers. Proc Natl Acad Sci USA 98:11857–11862
116. Smeenk JM, Otten MBJ, Thies J, Tirrell DA, Stunnenberg HG, van Hest JCM (2005) Controlled assembly of macromolecular β-Sheet fibrils. Angew Chem Int Ed 44:1968–1971
117. Choi YY, Joo MK, Sohn YS, Jeong B (2008) Significance of secondary structure in nanostructure formation and thermosensitivity of polypeptide block copolymers. Soft Matter 4:2383–2387
118. Choi YY, Jang JH, Park MH, Choi BG, Chi B, Jeong B (2010) Block length affects secondary structure, nanoassembly and thermosensitivity of poly(ethylene glycol)-poly(L-alanine) block copolymers. J Mater Chem 20:3416–3421
119. Petka WA, Harden JL, McGrath KP, Wirtz D, Tirrell DA (1998) Reversible hydrogels from self-assembling artificial proteins. Science 281:389–392
120. Eloi J-C, Rider DA, Cambridge G, Whittell GR, Winnik MA, Manners I (2011) Stimulus-responsive self-assembly: reversible, redox-controlled micellization of polyferrocenylsilane diblock copolymers. J Am Chem Soc 133:8903–8913
121. Ho R-M, Chiang Y-W, Lin S-C, Chen C-K (2011) Helical architectures from self-assembly of chiral polymers and block copolymers. Prog Polym Sci 36:376–453

122. Lin J, Zhu J, Chen T, Lin S, Cai C, Zhang L, Zhuang Y, Wang X-S (2009) Drug releasing behavior of hybrid micelles containing polypeptide triblock copolymer. Biomaterials 30:108–117
123. Fuks G, Mayap Talom R, Gauffre F (2011) Biohybrid block copolymers: towards functional micelles and vesicles. Chem Soc Rev 40:2475–2493
124. Qian J, Zhang M, Manners I, Winnik MA (2010) Nanofiber micelles from the self-assembly of block copolymers. Trends Biotechnol 28:84–92
125. Cauet SI, Lee NS, Lin LY, Wooley KL (2012) Individual nano-objects obtained via hierarchical assembly of polymer building blocks. In: Matyjaszewski K, Moller M (eds) Polymer science: a comprehensive reference. Elsevier, Amsterdam, pp 775–820
126. Feng C, Li Y, Yang D, Hu J, Zhang X, Huang X (2011) Well-defined graft copolymers: from controlled synthesis to multipurpose applications. Chem Soc Rev 40:1282–1295
127. Bian Q, Xiao Y, Lang M (2012) Thermoresponsive biotinylated star amphiphilic block copolymer: synthesis, self-assembly, and specific target recognition. Polymer 53:1684–1693
128. Cai C, Wang L, Lin J, Zhang X (2012) Morphology transformation of hybrid micelles self-assembled from rod-coil block copolymer and nanoparticles. Langmuir 28:4515–4524
129. Cai C, Zhu W, Chen T, Lin J, Tian X (2009) Synthesis and self-assembly behavior of amphiphilic polypeptide-based brush-coil block copolymers. J Polym Sci A Polym Chem 47:5967–5978
130. Koga T, Taguchi K, Kobuke Y, Kinoshita T, Higuchi M (2003) Structural regulation of a peptide-conjugated graft copolymer: a simple model for amyloid formation. Chem Eur J 9:1146–1156
131. Tang D, Lin J, Lin S, Zhang S, Chen T, Tian X (2004) Self-assembly of poly(γ-benzyl L-glutamate)-graft-poly(ethylene glycol) and its mixtures with poly(γ-benzyl L-glutamate) homopolymer. Macromol Rapid Commun 25:1241–1246
132. Marsden HR, Handgraaf J-W, Nudelman F, Sommerdijk NAJM, Kros A (2010) Uniting polypeptides with sequence-designed peptides: synthesis and assembly of poly (γ-benzyl L-glutamate)-b-coiled-coil peptide copolymers. J Am Chem Soc 132:2370–2377
133. Huang J, Bonduelle C, Thevenot J, Lecommandoux S, Heise A (2012) Biologically active polymersomes from amphiphilic glycopeptides. J Am Chem Soc 134:119–122
134. Checot F, Lecommandoux S, Gnanou Y, Klok HA (2002) Water-soluble stimuli-responsive vesicles from peptide-based diblock copolymers. Angew Chem Int Ed 41:1339–1343
135. Sun J, Chen X, Deng C, Yu H, Xie Z, Jing X (2007) Direct formation of giant vesicles from synthetic polypeptides. Langmuir 23:8308–8315
136. Schatz C, Louguet S, Le Meins J-F, Lecommandoux S (2009) Polysaccharide-block-polypeptide copolymer vesicles: towards synthetic viral capsids. Angew Chem Int Ed 48:2572–2575
137. Holowka EP, Sun VZ, Kamei DT, Deming TJ (2007) Polyarginine segments in block copolypeptides drive both vesicular assembly and intracellular delivery. Nat Mater 6:52–57
138. Cai C, Lin J, Chen T, Tian X (2010) Aggregation behavior of graft copolymer with rigid backbone. Langmuir 26:2791–2797
139. Zhuang Z, Zhu X, Cai C, Lin J, Wang L (2012) Self-assembly of a mixture system containing polypeptide graft and block copolymers: experimental studies and self-consistent field theory simulations. J Phys Chem B 116:10125–10134
140. Cornelissen JJLM, Fischer M, Sommerdijk NAJM, Nolte RJM (1998) Helical superstructures from charged poly(styrene)-poly(isocyanodipeptide) block copolymers. Science 280:1427–1430
141. Cai C, Lin J, Chen T, Wang X, Lin S (2009) Super-helices self-assembled from a binary system of amphiphilic polypeptide block copolymers and polypeptide homopolymers. Chem Commun 2709–2711
142. Bull SR, Palmer LC, Fry NJ, Greenfield M, Messmore B, Meade T, Stupp SI (2008) A templating approach for monodisperse self-assembled organic nanostructures. J Am Chem Soc 130:2742–2743